5-Alkyl-6-benzyl-2-(2-oxo-2-phenylethylsulfanyl)pyrimidin-4(3*H*)-ones, a Series of Anti-HIV-1 Agents of the Dihydro-alkoxy-benzyl-oxopyrimidine Family with Peculiar Structure−Activity Relationship Profile

Maxim B. Nawrozkij,[†,‡] Dante Rotili,[§,‡] Domenico Tarantino,[§] Giorgia Botta,[§,||] Alexandre S. Eremiychuk,[†] Ira Musmuca,[§] Rino Ragno,[§] Alberta Samuele,[⊥] Samantha Zanoli,[⊥] Mercedes Armand-Ugón,[#] Imma Clotet-Codina,[#] Ivan A. Novakov,[†] Boris S. Orlinson,[†] Giovanni Maga,[⊥] José A. Esté,[#] Marino Artico,[§] and Antonello Mai*[,§]

Volgograd State Technical University, Pr. Lenina, 28, 400131 Volgograd, Russia, Dipartimento di Studi Farmaceutici, Sapienza Università di Roma, P. le A. Moro 5, 00185 Roma, Italy, Istituto di Genetica Molecolare IGM-CNR, via Abbiategrasso 207, 27100 Pavia, Italy, and Retrovirology Laboratory IrsiCaixa, Hospital Universitari Germans Trias i Pujol, Universitat Autònoma de Barcelona, 08916 Badalona, Spain

Received March 26, 2008

A series of dihydro-alkylthio-benzyl-oxopyrimidines (*S*-DABOs) bearing a 2-aryl-2-oxoethylsulfanyl chain at pyrimidine C2, an alkyl group at C5, and a 2,6-dichloro-, 2-chloro-6-fluoro-, and 2,6-difluoro-benzyl substitution at C6 (oxophenethyl-*S*-DABOs, **6**−**8**) is here described. The new compounds showed low micromolar to low nanomolar (in one case subnanomolar) inhibitory activity against wt HIV-1. Against clinically relevant HIV-1 mutants (K103N, Y181C, and Y188L) as well as in enzyme (wt and K103N, Y181I, and L100I mutated RTs) assays, compounds carrying an ethyl/*iso*-propyl group at C5 and a 2,6-dichloro-/2-chloro-6-fluoro-benzyl moiety at C6 were the most potent derivatives, also characterized by low fold resistance ratio. Interestingly, the structure−activity relationship (SAR) data drawn from this DABO series are more related to HEPT than to DABO derivatives. These findings were at least in part rationalized by the description of a fair superimposition between the **6**−**8** and TNK-651 (a HEPT analogue) binding modes in both WT and Y181C RTs.

Introduction

Dihydro-alkoxy-benzyl-oxopyrimidines (DABOs)[1,2] are a family of non-nucleoside reverse transcriptase (RT) inhibitors (NNRTIs)[3–5] endowed with micromolar to subnanomolar activity against human immunodeficiency virus type 1 (HIV-1). We disclosed the first series of these inhibitors in 1992 by describing the synthesis and antiviral activity of a number of pyrimidin-4(3*H*)-ones bearing an alkoxy chain at the C2 position and a benzyl/3-methylbenzyl/3,5-dimethylbenzyl group at the C6 position of the pyrimidine ring (DABOs[a], Figure 1).[6–9] The replacement of the C2-alkoxy with a C2-alkylthio chain gave an increase of the antiviral potency of the derivatives, which showed submicromolar activity against wild type (wt) HIV-1 (*S*-DABOs, DATNOs; Figure 1).[10–12] In our hands, the introduction of a C6-naphthylmethyl moiety instead of the C6-benzyl one did not furnish a significant improvement of activity.[12] Differently, the substitution of the C6-benzyl ring with halogens (chloro, fluoro) at the 2- and 2,6-positions afforded highly potent compounds (F_2-*S*-DABOs, Figure 1), active at nanomolar concentration against wt HIV-1.[13–15] Conformational restriction applied to F_2-*S*-DABOs further improved the anti-HIV-1 activity of the derivatives, leading to compounds active at low nanomolar level against the wild type virus and also active against the HIV-1 Y181C mutant.[16–18] By replacing the C2-alkylthio with a C2-alkylamino moiety, two further series (F_2-*NH*-DABOs and F_2-*N,N*-DABOs, Figure 1) of highly potent, broad spectrum NNRTI compounds belonging to the DABO family have been obtained.[19–22]

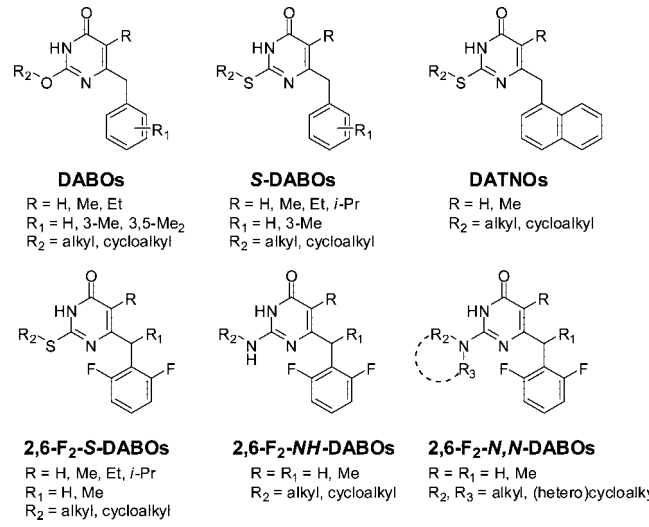

Figure 1. The DABO family.

In summary, we can draw the following structure−activity relationships (SAR) (Figure 2) about the DABO family to obtain

* To whom correspondence should be addressed. Phone: +396-4991-3392. Fax:+396-491491. E-mail:antonello.mai@uniroma1.it.

† Volgograd State Technical University.

‡ MBN and DR contributed equally to this work.

§ Sapienza Università di Roma.

|| Present address: Dipartimento Farmaco Chimico Tecnologico, Università degli Studi di Siena, via A. Moro, 53100 Siena, Italy.

⊥ Istituto di Genetica Molecolare IGM-CNR.

Universitat Autònoma de Barcelona.

[a] Abbreviation: AIDS, acquired immunodeficiency syndrome; BHAP, bis(heteroaryl)piperazine; CC_{50}, compound concentration toxic for 50% of cells; DABOs, dihydro-alkoxy-benzyl-oxopyrimidines; DATNOs, dihydro-alkylthio-naphthylmethyl-oxopyrimidines; EC_{50}, effective concentration able to protect 50% of cells from the HIV-1 induced cytopathogenicity; EFV, efavirenz; F_2-*N,N*-DABOs, 5-alkyl-2-(*N,N*-disubstituted)amino-6-(2,6-difluorophenylalkyl)pyrimidin-4(3*H*)ones; HEPT, 1-[(2-hydroxyethoxy)methyl]-6-(phenylthio)thymine; HIV, human immunodeficiency virus; MTT, 3-(4,5-dimethylthiazol-2-yl)-2,5-diphenyltetrazolium bromide; *NH*-DABOs, dihydro-alkylamino-benzyl-oxopyrimidines; NNBS, non-nucleoside binding site; NNRTIs, non-nucleoside reverse transcriptase inhibitors; NVP, nevirapine; PDB, protein data bank; RCSB, research collaboratory for structural bioinformatics; RT, reverse transcriptase; SAR, structure−activity relationship; *S*-DABOs, dihydro-alkylthio-benzyl-oxopyrimidines; WT, wild type.

10.1021/jm800340w CCC: $40.75
Published on Web 07/17/2008

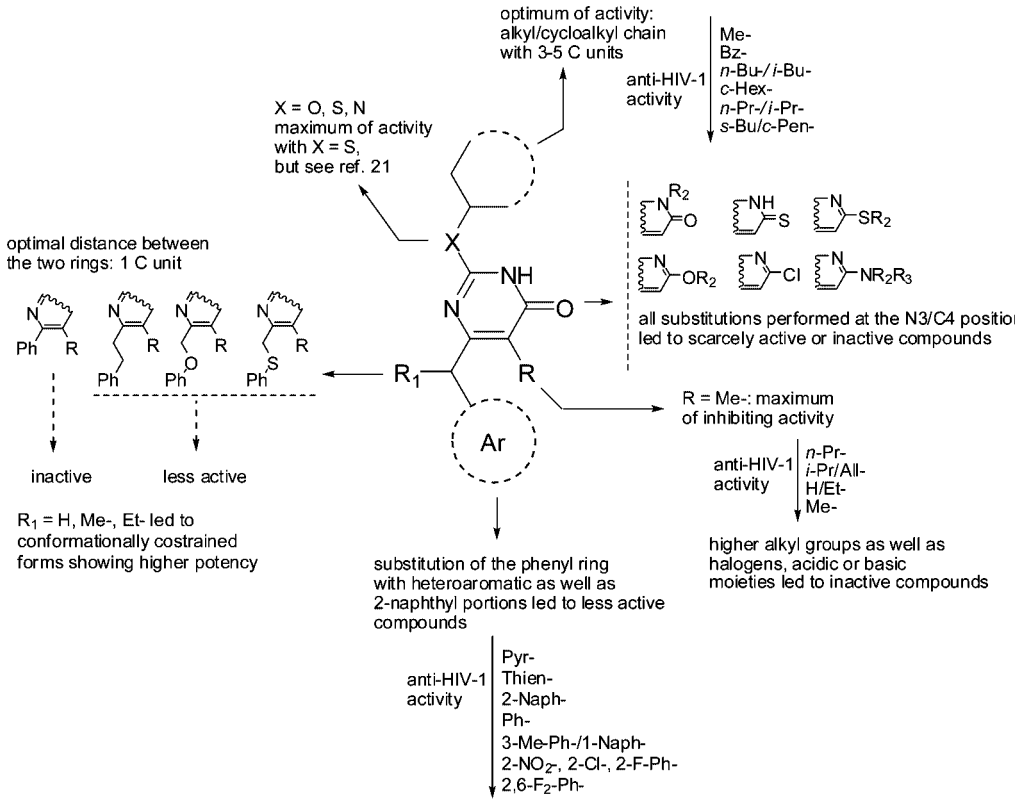

Figure 2. SAR graphical summary of DABOs.

the highest HIV-1 inhibitory activity: (i) The pyrimidin-4(3*H*)-one ring must carry a 2,6-difluoro-benzyl/-1-phenylethyl substituent at the C6 position, and a properly sized alkoxy, alkylthio, or alkylamino chain at the C2 position. (ii) The HNC═O fragment at N3/C4 position of the pyrimidine must be unchanged. (iii) With the exception of the methylthiomethyl-*S*-DABOs,[14] the C5 position of the pyrimidine has to be substituted with a methyl group (thymine derivatives): the uracil, 5-ethyluracil, and 5-*iso*-propyluracil derivatives are typically less potent than the corresponding thymines. These SAR are quite different from those of the DABO-related HEPT derivatives, in which, to display the highest anti-HIV-1 activity, the pyrimidine ring must be substituted with a 3,5-dimethylbenzyl moiety at C6 and a *iso*-propyl group at C5.[23–28]

As a rule, to insert the C2-alkoxy, -alkylthio, or -alkylamino chain in the DABO compounds, we linked either linear, branched, or cyclic alkyl moieties with a growing number of carbon units at the heteroatom at the C2 position of the pyrimidine ring. The highest inhibitory activity was registered with the insertion of *iso*-propyl, *n*-propyl, *sec*-butyl, *n*-butyl, or cyclopentyl chains. Examples of C2-aryl(alkyl)thio chains in the *S*-DABO series were performed by us (compounds **1a**−**p**, Figure 3), but the obtained compounds showed lower anti-HIV activity when compared with the corresponding C2-alkylthio counterparts (**1q**,**r**) (Table 1),[29] thus confirming the negative trend highlighted by Mugnaini et al. with some *S*-aryl-*S*-DABOs.[30]

In 2005, Manetti et al. reported that *S*-DABOs showing a 4-methoxybenzyl-/4-methoxyphenylethyl-thio substitution at C2, a methyl group at C5, and a 2,6-dichlorobenzyl moiety at C6 (**2** and **3**, Figure 3) displayed nanomolar to subnanomolar activity against both wt HIV-1 and the clinical isolate IRLL98 and micromolar/submicromolar activity against the HIV-1 K103N and Y188L mutant strains.[30] Very recently, the same group optimized their molecules by studying the effects of different substitution patterns at position 2, 5, and 6 of the pyrimidine ring.[31] The obtained new lead compound **4**, having a 4-methoxybenzylthio moiety at C2, a methyl group at C5, and a 1-(2,6-difluorophenylethyl) portion at C6, displayed picomolar activity against wt HIV-1 and submicromolar activities against some clinically relevant HIV-1 mutants.[31] In the same paper, four compounds having a phenacyl moiety at the sulfur atom at C2 of the pyrimidine ring have been reported, but they were endowed with low (if any) antiviral activity both against wt HIV-1 and mutant strains.[31] Moreover, a series of 5-alkyl-2-(2-aryl-2-oxoethylsulfanyl)-6-(1-naphthylmethyl)pyrimidin-4(3*H*)-ones was reported by He et al. as unique NNRTIs of the *S*-DABO series.[32,33] In these compounds, the highest activity (30 nM against wt HIV-1) has been obtained with the introduction of a 2-(4-methoxyphenyl)-2-oxoethylsulfanyl chain at the C2 position, and a *iso*-propyl group at the C5 position of the pyrimidine ring (**5**, Figure 3). However, limited data on the effects of such compounds against HIV mutant strains are available, and no data have been reported about RT inhibition.

From these findings, with the aim to acquire new SAR information and to explore the effect of the insertion of a C2-oxo-phenethylsulfanyl moiety in our *S*-DABOs, on the activity against wt HIV-1 and a panel of clinically relevant HIV-1 mutants, we prepared a further series of *S*-DABOs (oxophenethyl-*S*-DABOs **6**−**8**, Figure 3), characterized by the insertion of a 2-oxo-2-[(substituted)phenyl]ethylsulfanyl chain at C2, a 2,6-dichloro-, 2-chloro-6-fluoro-, or 2,6-difluorobenzyl group at C6, and hydrogen, methyl, ethyl, *iso*-propyl, or *sec*-butyl substituent at C5.

Chemistry. The ethyl arylacetylacetates **9a**−**l**, key intermediates for the synthesis of the title DABO derivatives, were prepared through two alternative routes. The 2-H- and 2-methyl-β-oxoesters **9a**,[13]**b**,[13]**e**,**f**,**j**,[13] were obtained by reaction of the appropriate acylimidazolide with potassium ethyl malonate and 2-methylmalonate in the presence of triethylamine and magne-

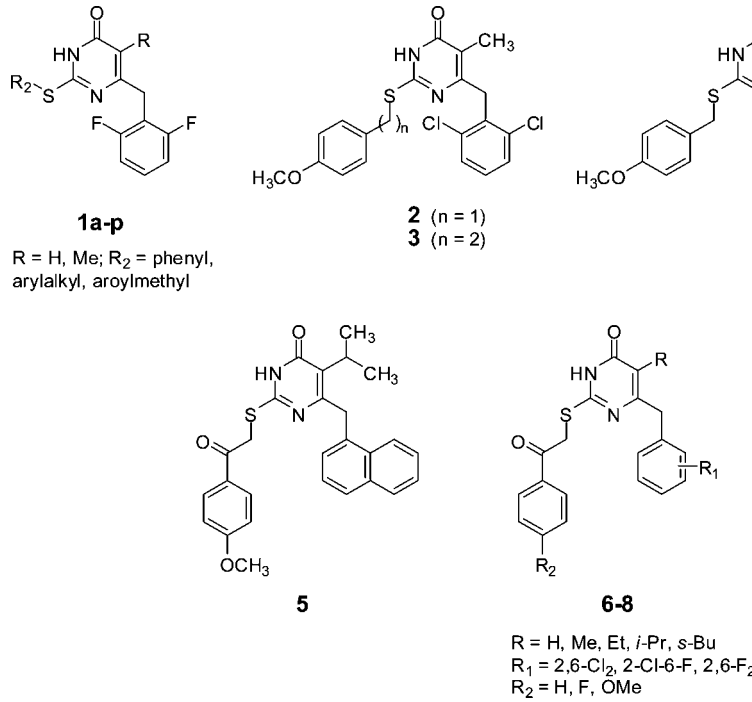

Figure 3. Arylalkyl-*S*-DABOs (**1**−**4**), 5-*iso*-propyl-2-[2-(4-methoxyphenyl)-2-oxoethylsulfanyl]-6-(1-naphthylmethyl)pyrimidin-4(3*H*)-one (oxophenethyl-DATNO, **5**), and oxophenethyl-*S*-DABOs (**6**−**8**).

Table 1. Cytotoxicity and Anti-HIV-1 Activity of Arylalkyl-F_2-*S*-DABOs **1a**−**p**[a]

compd	R	R_2	CC_{50},[b] μM	EC_{50},[c] μM	SI[d]
1a	H	Ph	>76[e]	1.4	>54
1b	H	$PhCH_2$	>73	0.1	>730
1c	H	2,6-F_2−$PhCH_2$	>66	1.0	>66
1d	H	$PhCH_2CH_2$	>70	0.3	>233
1e	H	$PhCH_2CH_2CH_2$	32	0.2	160
1f	H	CH_3COCH_2	>81	3.1	>26
1g	H	$PhCOCH_2$	>67	1.0	>67
1h	H	4-Cl-$PhCOCH_2$	>61	9.8	>6
1i	H	4-NO_2−$PhCOCH_2$	22	8.4	>3
1j	Me	$PhCH_2$	>70	0.13	>538
1k	Me	4-NO_2−$PhCH_2$	>37	1.2	>31
1l	Me	2,4-Me_2-$PhCH_2$	>65	0.4	>162
1m	Me	3,5-Me_2-$PhCH_2$	>65	14.0	>5
1n	Me	2-pyridyl-CH_2	>70	10.1	>7
1o	Me	3-pyridyl-CH_2	>70	5.9	>12
1p	Me	4-pyridyl-CH_2	>70	0.06	>1167
1q	H	*iso*-propyl	>84	0.017	4941
1r	Me	*iso*-propyl	>77	0.006	12833

[a] Values are means ± SD determined from at least two experiments. The alkylthio-substituted F_2-*S*-DABOs **1q**,**r** have been added for a direct comparison. [b] Cytotoxic concentration 50, concentration to induce 50% death of noninfected cells, evaluated with the MTT method in MT-4 cells. [c] Effective concentration 50, concentration needed to inhibit 50% HIV-induced cytopathic effect, evaluated with the MTT method in MT-4 cells (HIV-1 strain: NL4−3). [d] Selectivity index, CC_{50}/EC_{50}. [e] Higher concentrations could not be tested due to precipitation of compounds in the culture medium.

sium chloride, according to the previously reported simple and high-yielding method (Scheme 1, route a).[13] The 2-ethyl-, 2-*iso*-propyl-, and 2-*sec*-butyl-substituted β-oxoesters **9c**,**d**,**g**−**i**,**k**,[15]**l**[15] were obtained by a modified Blaise procedure involving the reaction between the proper arylacetonitriles and ethyl 2-bromobutanoate, 2-bromo-3-methylbutanoate, or 2-bromo-3-methylpentanoate[35] in the presence of freshly prepared zinc turnings, followed by acidic hydrolysis of the enamine intermediate (Scheme 1, route b). Further condensation of the β-oxoesters **9a**−**l** with thiourea in alkaline medium afforded the 5-alkyl-6-(2,6-dihalobenzyl)-2-thioxo-2,3-dihydropyrimidin-4(1*H*)-ones **10a**−**l**, which were alkylated with the proper ω-bromoacetophenones in the presence of sodium methoxide in methanol (route d, for **6** and **7**) or, alternatively, of potassium carbonate in *N*,*N*-dimethylformamide (route e, for **8**) to give the title compounds **6**−**8** (Scheme 1).

Chemical and physical data for compounds **6**−**10** are listed in Table 2.

Results and Discussion

Cytotoxicity and Wild Type HIV-1 Inhibiting Activity. The oxophenethyl-*S*-DABOs **6–8** were tested in MT-4 cells to evaluate their cytotoxicity and their capability to inhibit the HIV-induced cytopathic effect (HIV-1 strain: NL4−3) by 50%. Nevirapine (NVP) and efavirenz (EFZ) were also tested as reference drugs (Table 3).

The majority of the tested compounds were not cytotoxic up to 65 μM. Some compounds showed >11/>14 μM values of CC_{50} (compound concentration toxic for 50% of cells) because higher concentration could not be achieved for the precipitation of the compounds in the culture medium.

When tested against wt HIV-1, the uracils **6a**−**c** and **7a**−**c** displayed micromolar/submicromolar activity. With the insertion of an alkyl substituent at the C5 position of the pyrimidine, the inhibitory activity increased according to the order *iso*-propyl (*i*-Pr)/*sec*-butyl (*s*-Bu) > Et > Me. Differently from other DABO series, in which the optimal substituent at the C5 position was the methyl group[7,9,10,15,17,20,22,32] in oxophenethyl-*S*-DABOs, the thymine derivatives (**6d**−**f**, **7d**,**f**, **8a**−**c**) showed anti-HIV-1 activity in the high nanomolar range (200 to 15 nM), whereas the 5-ethyluracil analogues (**6g**,**h**, **7g**−**i**, **8d**−**f**) were more potent in inhibiting wt HIV-1 (EC_{50}, concentration needed to inhibit 50% HIV-induced cytopathic effect, values ranging from 20 to 5 nM). Exceptions to this rule were the 6-(2-choro-6-fluorobenzyl)-5-methylpyrimidin-4(3*H*)-one **7e**, which was more potent than the other thymines being active at 2 nM, and the 6-(2,6-dichlorobenzyl)-5-ethyl-2-[2-(4-methoxyphenyl)-2-oxoethylsulfanyl] derivative **6i**, which inhibited HIV-1 at

Scheme 1[a]

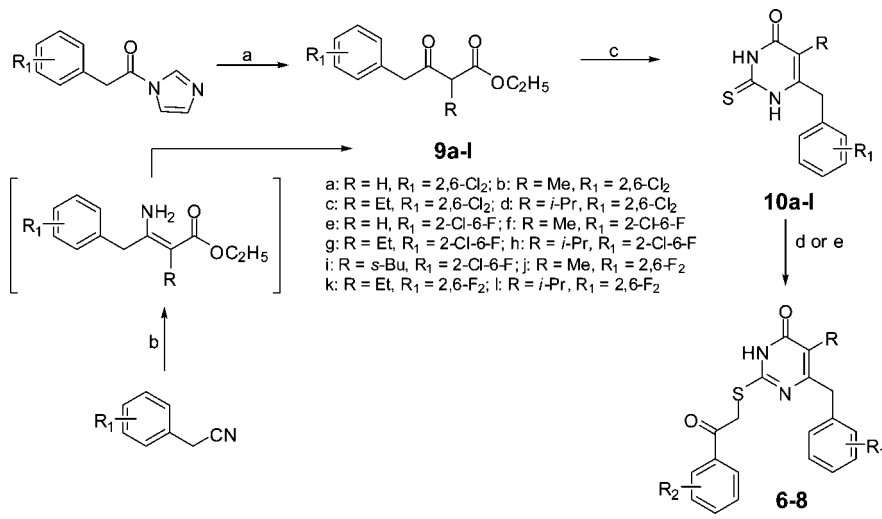

[a] (a) (1) KOOCCHRCOOEt, $MgCl_2$, Et_3N, CH_3CN, reflux; (2) 4 N HCl; (b) (1) RCH(Br)COOEt, Zn, THF, reflux; (2) 13% HCl, rt; (c) NH_2CSNH_2, EtOK, EtOH, reflux; (d) ω-bromoacetophenone, MeONa, MeOH, rt; (e) ω-bromoacetophenone, K_2CO_3, DMF, rt.

micromolar level. The 6-benzyl-5-*iso*-propyl-2-(2-oxo-2-phenylethylsulfanyl)pyrimidin-4(3*H*)-ones **6j**, **7j**−**l**, and **8g**−**i** as well as the 5-*sec*-butyl analogue **7n** were active at single-digit nanomolar concentration, and **6l** displayed anti-HIV-1 activity at subnanomolar level (EC_{50} = 0.4 nM).

The effect of halogen substitution of the C6-benzyl group in this series of compounds was different from other series of DABOs reported by us[13−15,17,20,22] and others.[30−32] In the compounds described herein, with some exceptions, the 5-ethyl/5-*iso*-propyl-2,6-dichlorobenzyl derivatives **6g**−**l** were more potent than the corresponding 2-chloro-6-fluoro- and 2,6-difluoro-analogues **7g**−**l** and **8d**−**i** in inhibiting wt HIV-1.

In oxophenethyl-*S*-DABOs, we introduced at C2 a 2-phenyl-, 2-(4-fluorophenyl)-, or 2-(4-methoxyphenyl)-2-oxoethylthio chain. We chose these substituents as they gave the highest anti-HIV activity to the 5-ethyl/5-*iso*-propyl-DATNO analogues reported by He et al.[33,34] Nevertheless, in our 2,6-Cl_2-, 2-Cl-6-F-, and 2,6-F_2-oxophenethyl-*S*-DABOs, the substituent at the *para*-position of the phenethyl moiety did not influence the inhibitory activity of the compounds, or only marginally. In some cases, the 4-methoxy (see for example **6l**, **7l**, and **8f**) and in others the 4-H and/or 4-F group (**6g**,**h**, **7e**,**h**, and **8a**,**b**) seem to be preferred.

Inhibitory Activity Against Clinically Relevant HIV-1 Mutant Strains. The oxophenethyl-*S*-DABOs **6**−**8** were also tested against a panel of clinically relevant HIV-1 mutants (K103N, Y181C, and Y188L) (Table 4). Among the three different substitutions studied in this work (at C5 position, R; at the C6-benzyl moiety, R_1; at the phenyl ring of the C2-oxophenethylsulfanyl chain, R_2), the insertion of a ethyl group at C5, a 2,6-dichloro- or 2-chloro-6-fluoro-benzyl portion at C6, and a unsubstituted 2-oxo-2-phenylethylsulfanyl chain at C2 seem to be suitable to obtain compounds highly active against the HIV-1 mutants. Indeed, high, wide-spectrum inhibitory activity was registered by the 6-(2,6-dichlorobenzyl)- and 6-(2-chloro-6-fluorobenzyl)-5-ethyl-2-(2-oxo-2-phenylethylsulfanyl)pyrimidin-4(3*H*)-ones **6g** and **7g** [$EC_{50}s^{K103N}$ (μM)/*fold resistance*: 1.2/*171* (**6g**) and 1.2/*100* (**7g**); $EC_{50}s^{Y181C}$: 0.046/*7* (**6g**) and 0.39/*32* (**7g**); $EC_{50}s^{Y188L}$: 5.0/*714* (**6g**) and 9.38/*782* (**7g**)]. The corresponding 5-*iso*-propyl analogues **6j** and **7j** showed low micromolar to submicromolar inhibition of the tested HIV-1 mutants but with higher fold resistance ratio [$EC_{50}s^{K103N}$ (μM)/*fold resistance*: 5.1/*1275* (**6j**) and 3.29/*658* (**7j**); $EC_{50}s^{Y181C}$ (μM)/*fold resistance*: 0.11/*27* (**6j**) and 0.21/*42* (**7j**); $EC_{50}s^{Y188L}$ (μM)/*fold resistance*: 5.5/*1375* (**6j**) and 7.7/*1540* (**7j**)]. The 6-(2,6-difluorobenzyl)-5-ethyl- and −5-*iso*-propyl counterparts **8d**,**g** showed good anti-HIV-1 activity against the K103N and Y181C mutants [$EC_{50}s^{K103N}$(μM)/*fold resistance*: 1.3/*108* (**7d**), and 4.46/*2230* (**7g**); $EC_{50}s^{Y181C}$(μM)/*fold resistance*: 0.2/*17* (**8d**) and 0.24/*120* (**8g**)] but were inactive against the Y188L mutant strain. The compound **6l**, active at subnanomolar level against wt HIV-1, was totally inefficient in inhibiting the K103N and Y188L virus strains and retained its activity only against Y181C but with a large loss of potency. The insertion of a 4-fluoro or a 4-methoxy substituent at the C2-oxophenethyl moiety gave in all cases a drastic reduction joined to a high fold-resistance ratio, or a total loss of activity of the compounds against the tested HIV-1 mutants.

Enzyme Inhibiting Activity: Effect on HIV-1 RT Wild type and NNRTI-resistant Mutants. The oxophenethyl-*S*-DABOs **6**−**8** were tested against recombinant wt HIV-1 RT as well as against a panel of recombinant RTs carrying known NNRTI-resistance mutations (K103N, Y181I, and L100I) (Table 5). As observed in in-cell tests, the SAR data drawn from our previously reported DABOs are not applicable to the oxophenethyl compounds. In the wt RT assay, the highest activity of the derivatives is associated with a *iso*-propyl > ethyl > H > methyl substitution at C5, and with the introduction of a 2-chloro-6-fluoro- > 2,6-dichloro- > 2,6-difluorobenzyl moiety at C6. As in cellular assays, also in enzyme tests the differently substituted chains at C2 showed only weak modulation of the inhibitory activity. The most potent wt RT inhibitory action was displayed by **7l**, which showed ID_{50} (inhibitory dose 50, compound dose required to inhibit the HIV-1 rRT activity by 50%) = 0.7 nM. Optimal, single-digit nanomolar activities were registered by the 6-(2-chloro-6-fluorobenzyl) derivatives **7a**, **7g**, **7i**, **7j**, and **7n** as well as by the 2,6-difluorobenzyl analogue **8g**. Nevertheless, when tested against the mutated RTs, such compounds retained in part their activities but together with high fold resistance ratio (**7a**, **7j**, **7n**, and **8g**), or were active against only one mutated RT (**7g** and **7i**). Differently, the 6-(2,6-dichlorobenzyl)-5-ethyl-2-(2-phenyl-2-oxoethylsulfanyl)pyrimidin-4(3*H*)-ones **6g**−**i**, which showed ID_{50} values against wt RT ranging from 71 to 23 nM, displayed low micromolar to

Table 2. Physical and Chemical Data for Compounds **6**−**10**

compd	R	R_1	R_2	mp (°C)	recryst solvent[a]	synth method[b]	% yield	formula[c]
6a	H	2,6-Cl_2	H	204–205	A	d	87	$C_{19}H_{14}Cl_2N_2O_2S$
6br	H	2,6-Cl_2	F	207–209	A	d	86	$C_{19}H_{13}Cl_2FN_2O_2S$
6c	H	2,6-Cl_2	OMe	219–220.5	A	d	75	$C_{20}H_{16}Cl_2N_2O_3S$
6d	Me	2,6-Cl_2	H	205–206	A	d	76	$C_{20}H_{16}Cl_2N_2O_2S$
6e	Me	2,6-Cl_2	F	220.5–221.5	B	d	56	$C_{20}H_{15}Cl_2FN_2O_2S$
6f	Me	2,6-Cl_2	OMe	239.5–240	A	d	72	$C_{21}H_{18}Cl_2N_2O_3S$
6g	Et	2,6-Cl_2	H	200.5–201.5	A	d	70	$C_{21}H_{18}Cl_2N_2O_2S$
6h	Et	2,6-Cl_2	F	225.5–227	A	d	79	$C_{21}H_{17}Cl_2FN_2O_2S$
6i	Et	2,6-Cl_2	OMe	234–235	B	d	59	$C_{22}H_{20}Cl_2N_2O_3S$
6j	*i*-Pr	2,6-Cl_2	H	210.5–211.5	B	d	65	$C_{22}H_{20}Cl_2N_2O_2S$
6k	*i*-Pr	2,6-Cl_2	F	229–230	B	d	54	$C_{22}H_{19}Cl_2FN_2O_2S$
6l	*i*-Pr	2,6-Cl_2	OMe	219–211	B	d	63	$C_{23}H_{22}Cl_2N_2O_3S$
7a	H	2-Cl-6-F	H	201–204.5	A	d	86	$C_{19}H_{14}ClFN_2O_2S$
7b	H	2-Cl-6-F	F	200–201	A	d	82	$C_{19}H_{13}ClF_2N_2O_2S$
7c	H	2-Cl-6-F	OMe	229–230.5	A	d	78	$C_{20}H_{16}ClFN_2O_3S$
7d	Me	2-Cl-6-F	H	191.5–194.5	B	d	59	$C_{20}H_{16}ClFN_2O_2S$
7e	Me	2-Cl-6-F	F	203.5–204.5	A	d	70	$C_{20}H_{15}ClF_2N_2O_2S$
7f	Me	2-Cl-6-F	OMe	236.5–238	A	d	73	$C_{21}H_{18}ClFN_2O_3S$
7g	Et	2-Cl-6-F	H	189–190.5	B	d	56	$C_{21}H_{18}ClFN_2O_2S$
7h	Et	2-Cl-6-F	F	210–211	A	d	79	$C_{21}H_{17}ClF_2N_2O_2S$
7i	Et	2-Cl-6-F	OMe	222.5–225.5	A	d	69	$C_{22}H_{20}ClFN_2O_3S$
7j	*i*-Pr	2-Cl-6-F	H	190.5–196	B	d	51	$C_{22}H_{20}ClFN_2O_2S$
7k	*i*-Pr	2-Cl-6-F	F	223–224	B	d	48	$C_{22}H_{19}ClF_2N_2O_2S$
7l	*i*-Pr	2-Cl-6-F	OMe	190–195	B	d	64	$C_{23}H_{22}ClFN_2O_3S$
7m	*s*-Bu	2-Cl-6-F	F	208.5–209.5	B	d	61	$C_{23}H_{21}ClF_2N_2O_2S$
7n	*s*-Bu	2-Cl-6-F	OMe	196.5–197.5	A	d	83	$C_{24}H_{24}ClFN_2O_3S$
8a	Me	2,6-F_2	H	215–218	C	e	84	$C_{20}H_{16}F_2N_2O_2S$
8b	Me	2,6-F_2	F	219–221	D	e	80	$C_{20}H_{15}F_3N_2O_2S$
8c	Me	2,6-F_2	OMe	222–224	D	e	76	$C_{21}H_{18}F_2N_2O_3S$
8d	Et	2,6-F_2	H	194–196	D	e	78	$C_{21}H_{18}F_2N_2O_2S$
8e	Et	2,6-F_2	F	206–208	D	e	77	$C_{21}H_{17}F_3N_2O_2S$
8f	Et	2,6-F_2	OMe	228–230	D	e	72	$C_{22}H_{20}F_2N_2O_3S$
8g	*i*-Pr	2,6-F_2	H	221–223	D	e	70	$C_{22}H_{20}F_2N_2O_2S$
8h	*i*-Pr	2,6-F_2	F	234–237	D	e	73	$C_{22}H_{19}F_3N_2O_2S$
8i	*i*-Pr	2,6-F_2	OMe	187–191	D	e	67	$C_{23}H_{22}F_2N_2O_3S$
9c	Et	2,6-Cl_2		oil		b	65	$C_{14}H_{16}Cl_2O_3$
9d	*i*-Pr	2,6-Cl_2		oil		b	62	$C_{15}H_{18}Cl_2O_3$
9e	H	2-Cl-6-F		48–50	E	a	92	$C_{12}H_{12}ClFO_3$
9f	Me	2-Cl-6-F		oil		a	78	$C_{13}H_{14}ClFO_3$
9g	Et	2-Cl-6-F		oil		b	72	$C_{14}H_{16}ClFO_3$
9h	*i*-Pr	2-Cl-6-F		oil		b	93	$C_{15}H_{18}ClFO_3$
9i	*s*-Bu	2-Cl-6-F		oil		b	76	$C_{16}H_{20}ClFO_3$
10c	Et	2,6-Cl_2		270–271	F	c	81	$C_{13}H_{12}Cl_2N_2OS$
10d	*i*-Pr	2,6-Cl_2		262–264	F	c	57	$C_{14}H_{14}Cl_2N_2OS$
10e	H	2-Cl-6-F		268–270.5	G	c	78	$C_{11}H_8ClFN_2OS$
10f	Me	2-Cl-6-F		243–244 dec	F	c	84	$C_{12}H_{10}ClFN_2OS$
10g	Et	2-Cl-6-F		228–230	F	c	31	$C_{13}H_{12}ClFN_2OS$
10h	*i*-Pr	2-Cl-6-F		240–242	F	c	32	$C_{14}H_{14}ClFN_2OS$
10i	*s*-Bu	2-Cl-6-F		217–219	H	c	21	$C_{15}H_{16}ClFN_2OS$

[a] A: ethanol/*N,N*-dimethylformamide; B: 2-propanol/ *N,N*-dimethylformamide; C: methanol; D: acetonitrile/tetrahydrofuran; E: *n*-hexane; F: ethanol; G: glacial acetic acid; H: acetonitrile. [b] See Scheme 1. [c] Analytic results were within ± 0.40% of the theoretical values.

submicromolar activities against K103N, Y181I, and L100I mutated RTs, without large loss of activity [$ID_{50}s^{K103N}$ (μM)/*fold resistance*: 1.88/*26* (**6g**), 1.79/*43* (**6h**), 0.48/*21* (**6i**); $ID_{50}s^{Y181I}$ (μM)/*fold resistance*: 0.33/*5* (**6g**), 0.24/*6* (**6h**), 0.14/*6* (**6i**); $ID_{50}s^{L100I}$ (μM)/*fold resistance*: 3.54/*50* (**6g**), 1.82/*43* (**6h**), 2.42/*105* (**6i**)].

Molecular Modeling and Binding Mode Studies. In previous molecular modeling studies, we described the putative binding modes of F_2-*S*-DABOs and F_2-*NH*-DABOs,[19,20] highlighting the differences with the experimental bound conformation of TNK-651 (Figure 4), a potent HEPT analogue,[36] in both WT and Y181C HIV-1 RTs. In the oxophenethyl-*S*-DABOs **6**−**8** reported here, we noted a peculiar SAR profile of activity more related to HEPT derivatives than to DABOs. Thus, we compared the binding modes of **6**−**8** with those of TNK-651 in WT (PDB[37] entry code 1RT2),[36] Y181C (PDB entry code 1JLA),[38] and L100I (PDB entry code 1S1V)[39] RTs by the means of Autodock 4.0.1.[40] About TNK-651, the analysis of the experimental binding modes revealed that substantially the overall binding mode is not influenced by the Y181C or L100I mutation (Figure S1 in Supporting Information). Furthermore, in the three RT isoforms (1RT2, 1JLA, and 1S1V) it is possible to identify at least five important binding regions (Figure 5): (1) a C5-*iso*-propyl binding pocket (red colored area in Figure 5), formed by the side-chain of Val179 and the backbone atoms of Tyr181, Val189, and Gly190, (2) a π-rich hydrophobic region [side-chains of Leu100 (Ile100), Tyr181 (Cys181), Tyr188, Phe227, Trp229, and Leu234], hosting the TNK-651 C6-benzyl moiety (blue colored area in Figure 5), (3) a short hydrophobic channel [one entrance of the non nucleoside binding site (NNBS), green-colored area in Figure 5], in which the −CH_2−O-CH_2− part of the TNK-651 N1-benzyloxymethyl chain makes interaction mainly with the terminal part of the Val106 and Tyr318 side chains, (4) the end of the NNBS entrance channel (purple-colored area in Figure 5), in which the side chain of Pro236 interacts with the benzyloxy portion of TNK-651, and (5) a H-bonding hydrophilic region (cyan-colored area in Figure 5), in which the backbone amido oxygen of Lys101 makes an

Table 3. Cytotoxicity and Anti-HIV-1 Activity (wt HIV-1 Strain: NL4-3) of **6**−**8**[a]

compd	R	R_1	R_2	CC_{50},[b] μM	EC_{50},[c] μM	selectivity index[d]
6a	H	2,6-Cl_2	H	>12[e]	1.78	>7
6b	H	2,6-Cl_2	F	>59	0.78	>76
6c	H	2,6-Cl_2	OMe	>11	1.22	>9
6d	Me	2,6-Cl_2	H	>60	0.038	>1579
6e	Me	2,6-Cl_2	F	>57	0.046	>1239
6f	Me	2,6-Cl_2	OMe	>56	0.067	>836
6g	Et	2,6-Cl_2	H	>52	0.007	>7429
6h	Et	2,6-Cl_2	F	>55	0.007	>7857
6i	Et	2,6-Cl_2	OMe	>54	3.3	>16
6j	*i*-Pr	2,6-Cl_2	H	>56	0.004	>14000
6k	*i*-Pr	2,6-Cl_2	F	>54	0.064	>844
6l	*i*-Pr	2,6-Cl_2	OMe	>14	0.0004	>35000
7a	H	2-Cl-6-F	H	>13	1.26	>10
7b	H	2-Cl-6-F	F	>61	0.29	>210
7c	H	2-Cl-6-F	OMe	>12	1.55	>8
7d	Me	2-Cl-6-F	H	>12	0.045	>267
7e	Me	2-Cl-6-F	F	>59	0.002	>29500
7f	Me	2-Cl-6-F	OMe	>12	0.2	>60
7g	Et	2-Cl-6-F	H	>12	0.012	>1000
7h	Et	2-Cl-6-F	F	>57	0.005	>11400
7i	Et	2-Cl-6-F	OMe	>11	0.02	>550
7j	*i*-Pr	2-Cl-6-F	H	>12	0.005	>2400
7k	*i*-Pr	2-Cl-6-F	F	>56	0.004	>14000
7l	*i*-Pr	2-Cl-6-F	OMe	>11	0.001	>11000
7m	*s*-Bu	2-Cl-6-F	F	>54	0.017	>3177
7n	*s*-Bu	2-Cl-6-F	OMe	40	0.006	>6667
8a	Me	2,6-F_2	H	65	0.015	4333
8b	Me	2,6-F_2	F	>62	0.025	>2480
8c	Me	2,6-F_2	OMe	>60	0.048	>1250
8d	Et	2,6-F_2	H	56	0.012	4667
8e	Et	2,6-F_2	F	>60	0.019	>3158
8f	Et	2,6-F_2	OMe	>58	0.009	>6444
8g	*i*-Pr	2,6-F_2	H	>60	0.002	>30000
8h	*i*-Pr	2,6-F_2	F	>58	0.005	>11600
8i	*i*-Pr	2,6-F_2	OMe	33	0.002	16500
2[f]				32	0.007	4571
3[f]				>57	<0.00014	>407143
4[g]				>12.4	0.000025	>496000
5[h]				203	0.030	6766
NVP				>7	0.13	>54
EFZ				>3	0.007	>429

[a] Values are means ± SD determined from at least three experiments. [b] Cytotoxic concentration 50, concentration to induce 50% death of noninfected cells, evaluated with the MTT method in MT-4 cells. [c] Effective concentration 50, concentration needed to inhibit 50% HIV-induced cytopathic effect, evaluated with the MTT method in MT-4 cells (HIV-1 strain: NL4−3). [d] Selectivity index, CC_{50}/EC_{50}. [e] Higher concentrations could not be tested due to precipitation of compounds in the culture medium. [f] Ref 31. [g] Ref 32. [h] Ref 33.

Table 4. Anti-HIV-1 Activity of **6-8** against Clinically Relevant HIV-1 Mutant Strains[a]

				EC_{50},[b] μM (*fold resistance*)[c]		
compd	R	R_1	R_2	K103N	Y181C	Y188L
6a	H	2,6-Cl_2	H	>12	>12	>12
6b	H	2,6-Cl_2	F	>59	>59	>59
6c	H	2,6-Cl_2	OMe	>11	>11	>11
6d	Me	2,6-Cl_2	H	3.79 *(100)*	0.48 *(13)*	8.82 *(232)*
6e	Me	2,6-Cl_2	F	>57	>57	>57
6f	Me	2,6-Cl_2	OMe	>56	1.2 *(18)*	>56
6g	Et	2,6-Cl_2	H	1.2 *(171)*	0.046 *(7)*	5.0 *(714)*
6h	Et	2,6-Cl_2	F	4.7 *(671)*	0.49 *(70)*	36.3 *(5186)*
6i	Et	2,6-Cl_2	OMe	>54	24.1 *(7)*	>54
6j	*i*-Pr	2,6-Cl_2	H	5.1 *(1275)*	0.11 *(27)*	5.5 *(1375)*
6k	*i*-Pr	2,6-Cl_2	F	>54	>54	>54
6l	*i*-Pr	2,6-Cl_2	OMe	>14	0.23 *(575)*	>14
7a	H	2-Cl-6-F	H	>13	>13	>13
7b	H	2-Cl-6-F	F	>61	13.9 *(48)*	>61
7c	H	2-Cl-6-F	OMe	>12	>12	>12
7d	Me	2-Cl-6-F	H	9.48 *(211)*	1.68 *(37)*	>12
7e	Me	2-Cl-6-F	F	8.72 *(4360)*	0.28 *(140)*	>59
7f	Me	2-Cl-6-F	OMe	>12	1.57 *(8)*	>12
7g	Et	2-Cl-6-F	H	1.2 *(100)*	0.39 *(32)*	9.38 *(782)*
7h	Et	2-Cl-6-F	F	4.14 *(828)*	1.93 *(386)*	>57
7i	Et	2-Cl-6-F	OMe	4.16 *(208)*	0.84 *(42)*	>11
7j	*i*-Pr	2-Cl-6-F	H	3.29 *(658)*	0.21 *(42)*	7.7 *(1540)*
7k	*i*-Pr	2-Cl-6-F	F	>56	0.56 *(140)*	>55
7l	*i*-Pr	2-Cl-6-F	OMe	>11	0.16 *(160)*	>11
7m	*s*-Bu	2-Cl-6-F	F	>54	0.86 *(51)*	>54
7n	*s*-Bu	2-Cl-6-F	OMe	>40	>40	>40
8a	Me	2,6-F_2	H	19 *(1267)*	0.52 *(35)*	>65
8b	Me	2,6-F_2	F	>62	0.35 *(14)*	>62
8c	Me	2,6-F_2	OMe	>60	0.65 *(13)*	>60
8d	Et	2,6-F_2	H	1.3 *(108)*	0.2 *(17)*	>56
8e	Et	2,6-F_2	F	5.14 *(270)*	0.72 *(38)*	>60
8f	Et	2,6-F_2	OMe	>58	0.25 *(28)*	>58
8g	*i*-Pr	2,6-F_2	H	4.46 *(2230)*	0.24 *(120)*	>60
8h	*i*-Pr	2,6-F_2	F	>58	0.18 *(36)*	>58
8i	*i*-Pr	2,6-F_2	OMe	17.5 *(8750)*	0.067 *(33)*	14.7 *(7350)*
2[d]				4.7 *(671)*	ND	>32
3[d]				0.87 *(6214)*	ND	6.9 *(49286)*
4[e]				0.55 *(22000)*	0.30 *(12000)*	0.95 *(38000)*
NVP				4.96 *(38)*	>7	>7
EFZ				0.39 *(56)*	0.044 *(6)*	1.57 *(224)*

[a] Values are means ± SD determined from at least two experiments. [b] Effective concentration 50, concentration needed to inhibit 50% HIV-induced cytopathic effect, evaluated with the MTT method in MT-4 cells. [c] Fold resistance: ratio of EC_{50} value against drug-resistant strain and EC_{50} of the wt NL4−3 strain strain (Table 3). [d] Ref 31. [e] Ref 32.

hydrogen bond with most of the RT cocrystallized NNRTIs (not-shown). The inspection of the Autodock-proposed binding modes of the oxophenethyl-*S*-DABOs **6**−**8** revealed a fair superimposition to those of TNK-651 both in WT and Y181C RTs, showing an overall common binding conformation (Figure 6 and Figure S2 in Supporting Information). It is noteworthy to underline that, in the WT RT structure, all the **6**−**8** derivatives share the same binding mode (part A of Figure S2 of the Supporting Information) whereas in the Y181C RT, although they are still highly superimposable (part B of Figure S2 of the Supporting Information), the various compounds display some influence of the Tyr181 → Cys181 mutation, so that the structure-based aligned conformations are slightly less overlapped. The mutation Leu100 → Ile100 seems to be detrimental for the conservation of such a binding (part C of Figure 6 and part C of Figure S2 of the Supporting Information). Indeed, the **6**−**8** bound conformations into the L100I RT (part C of Figure S2 of the Supporting Information) are somehow disordered, and there is not any common binding mode. It seems likely that the Leu → Ile mutation on one hand led to a wider NNBS space (part left of Figure S3 in Supporting Information), with some loss of ligand stabilizing interactions. On the other hand, in L100I, there is a new methyl group (of the Ile100 *sec*-butyl moiety) that in some cases clashes against the *S*-DABO pyrimidine ring, thus not allowing for the oxophenethyl-*S*-DABO compounds to keep their WT or Y181C binding modes (right part of of Figure S3 of the Supporting Information). Interestingly, the docked conformations of almost the all C5-ethyl substituted compounds (**6g**, **6h**, **6i**, **7g**, **7h**, **7i**, **8d**, and **8e**) revealed a limited influence of the L100I mutation, and this is, at least in part, in agreement with their activity profile (see Table 5).

Somehow, the bound conformations of **6g**, **6h**, **6i**, **7g**, **7h**, **7i**, **8d**, and **8e** place the plane of the pyrimidine ring at a positive contributing Lennard-Jones interaction with the Ile100 *sec*-butyl methyl (Figure S4 in Supporting Information) and retain the WT or Y181C binding mode.

The introduction of the 2-oxo-2-phenylethyl group is definitely one important feature of the oxophenethyl-*S*-DABOs. The inspection of their docked conformations in either the WT or Y181C RTs revealed that the carbonyl oxygen makes an hydrogen bond interaction with Lys103 amide NH, which could explain the decreased anti-HIV potency against the clinically relevant K103N mutant strain as the Lys103 → Asn103 mutation

Table 5. Inhibitory Activity of **6-8** against HIV-1 RT Wild Type and NNRTI-Resistant Mutants[a]

				ID_{50},[b] μM (*fold resistance*)[c]			
compd	R	R_1	R_2	WT	K103N	Y181I	L100I
6a	H	2,6-Cl_2	H	0.012	3.7 *(308)*	0.26 *(22)*	11.0 *(917)*
6b	H	2,6-Cl_2	F	0.21	9.7 *(46)*	9.7 *(46)*	26.1 *(124)*
6c	H	2,6-Cl_2	OMe	0.054	37.5 *(694)*	0.11 *(2)*	>40
6d	Me	2,6-Cl_2	H	0.23	12.0 *(53)*	1.38 *(6)*	7.8 *(34)*
6e	Me	2,6-Cl_2	F	0.19	>40	0.8 *(4)*	10.7 *(56)*
6f	Me	2,6-Cl_2	OMe	0.094	>40	0.46 *(5)*	>40
6g	Et	2,6-Cl_2	H	0.071	1.88 *(26)*	0.33 *(5)*	3.54 *(50)*
6h	Et	2,6-Cl_2	F	0.042	1.79 *(43)*	0.24 *(6)*	1.82 *(43)*
6i	Et	2,6-Cl_2	OMe	0.023	0.48 *(21)*	0.14 *(6)*	2.42 *(105)*
6j	*i*-Pr	2,6-Cl_2	H	0.031	27.7 *(894)*	16.8 *(542)*	10.1 *(326)*
6k	*i*-Pr	2,6-Cl_2	F	0.020	ND[d]	30.6 *(1530)*	ND
6l	*i*-Pr	2,6-Cl_2	OMe	0.014	>40	17.1 *(1221)*	>40
7a	H	2-Cl-6-F	H	0.002	2 *(1000)*	0.4 *(200)*	1.5 *(750)*
7b	H	2-Cl-6-F	F	0.93	20.7 *(22)*	9.2 *(10)*	>40
7c	H	2-Cl-6-F	OMe	0.014	3.4 *(243)*	>40	0.5 *(36)*
7d	Me	2-Cl-6-F	H	0.012	23.0 *(1917)*	1.2 *(100)*	3.3 *(275)*
7e	Me	2-Cl-6-F	F	0.18	5.35 *(30)*	0.7 *(4)*	8.8 *(49)*
7f	Me	2-Cl-6-F	OMe	0.018	2.7 *(150)*	1.2 *(67)*	25.0 *(1389)*
7g	Et	2-Cl-6-F	H	0.008	>40	>40	9.7 *(1213)*
7h	Et	2-Cl-6-F	F	0.033	1.64 *(50)*	0.38 *(12)*	5.6 *(170)*
7i	Et	2-Cl-6-F	OMe	0.007	>40	>40	2.9 *(414)*
7j	*i*-Pr	2-Cl-6-F	H	0.001	4.5 *(4500)*	>40	1.3 *(1300)*
7k	*i*-Pr	2-Cl-6-F	F	0.024	40 *(1667)*	>40	ND
7l	*i*-Pr	2-Cl-6-F	OMe	0.0007	>40	>40	>40
7m	*s*-Bu	2-Cl-6-F	F	0.024	>40	>40	32.7 *(1363)*
7n	*s*-Bu	2-Cl-6-F	OMe	0.007	0.59 *(84)*	7.9 *(1129)*	27.4 *(3914)*
8a	Me	2,6-F_2	H	0.33	10.4 *(32)*	1.68 *(5)*	12.7 *(38)*
8b	Me	2,6-F_2	F	0.41	12.0 *(29)*	1.71 *(4)*	39.2 *(96)*
8c	Me	2,6-F_2	OMe	0.26	22.7 *(87)*	1.17 *(4)*	>40
8d	Et	2,6-F_2	H	0.043	3.7 *(86)*	0.82 *(19)*	5.4 *(126)*
8e	Et	2,6-F_2	F	0.061	3.65 *(60)*	0.51 *(8)*	6.9 *(113)*
8f	Et	2,6-F_2	OMe	0.031	3.41 *(110)*	0.58 *(19)*	>40
8g	*i*-Pr	2,6-F_2	H	0.008	1.58 *(198)*	>40	4.8 *(600)*
8h	*i*-Pr	2,6-F_2	F	0.082	5.82 *(71)*	>40	5.7 *(70)*
8i	*i*-Pr	2,6-F_2	OMe	0.026	37.3 *(1435)*	>40	>40
2[e]				0.004	102 *(25500)*	150 *(37500)*	ND
3[e]				0.026	3.2 *(123)*	1.5 *(58)*	ND
4[f]				0.003	45 *(15000)*	>20	ND
NVP				0.4	7 *(17)*	35 *(87)*	9 *(22)*
EFZ				0.03	3 *(100)*	0.08 *(3)*	ND

[a] Values are means ± SD determined from at least three experiments. [b] Inhibitory dose 50, compound dose required to inhibit the HIV-1 rRT activity by 50%. [c] Fold resistance: ratio of ID_{50}mut/ID_{50}wt values. [d] ND, not determined. [e] Ref 31. [f] Ref 32.

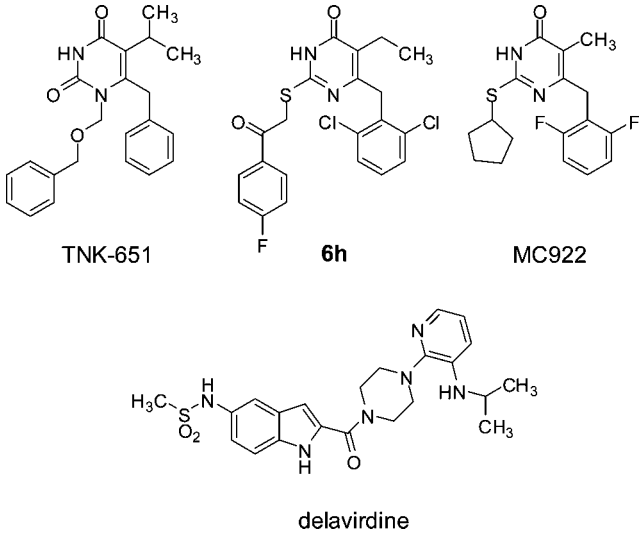

Figure 4. Structures of the NNRTIs used for molecular modeling studies.

involve movement of the whole 103 residue and therefore ligand interactions with this amino acid are likely diminished. At the same time, the new hydrogen bonding interaction seems to face the influence of the Y181C mutation, as it represents a further anchor point that fill the loss introduced by the Tyr181 → Cys181 mutation, similarly to that previously reported for the *NH*-DABOs.[19,20] As a additional proof of the importance of the introduced feature, docking experiments were also carried out on the reported F_2-*S*-DABO MC922[13] (Figure 4) in comparison with **6**−**8**. The docked conformation of MC922 clearly show that the position of the pyrimidine ring is somehow slightly shifted toward the top of the red-colored region in respect to the average position of the **6**−**8** as well as to the TNK-651 pyrimidine (Figure 7). Thus, the C5-methyl of MC922 is neither overlapped with the C5-substituent of **6**−**8** nor with the C5-*iso*-propyl group of TNK-651 (red-colored region). This is in agreement with the herein reported SAR profile, in which an increase of bulkiness at the pyrimidine C5 position led to more active oxophenethyl-*S*-DABO derivatives, differently from that observed with the F_2-*S*-DABOs. Furthermore, a direct comparison to the TNK-651 and delavirdine (a well-known NNRTI approved for therapy, Figure 4, PDB entry code 1KLM)[41] bound conformations (WT RT structures) highlighted that the oxophenethyl-*S*-DABOs showed a sort of mixed TNK-651/delavirdine structural profile (Figure S5 in Supporting Information). This last observation could be useful to design novel series of NNRTIs through the building of a sort of chimera between HEPT, DABO, and bis(heteroaryl)piperazine (BHAP) compounds (Figure S6 in Supporting Information).

Conclusion

In this paper, a further series of *S*-DABOs, the oxophenethyl-*S*-DABOs **6**−**8** have been reported as NNRTIs active against wt HIV-1 (NL4−3 strain) as well as a panel of clinically relevant HIV-1 mutant strains (K103N, Y181C, and Y188L). Despite the fact that they belong to the DABO family, in both cellular and enzyme assays, the oxophenethyl-*S*-DABO compounds showed SAR data deeply different from those typical of the DABO family. In particular, to obtain the highest wide spectrum anti-HIV-1 activity, it seems to be important to insert an ethyl/*iso*-propyl group at the C5 position of the pyrimidine ring, and a 2,6-dichlorobenzyl/2-chloro-6-fluorobenzyl moiety at the C6 position. The 6-(2,6-dichlorobenzyl)-5-ethyl-2-(2-oxo-2-phenylethylsulfanyl)pyrimidin-4(3*H*)-one **6g** was one of the compounds endowed with the highest broad spectrum HIV-1 inhibitory activity, with EC_{50} = 7 nM against the wt virus, EC_{50} = 46 nM against the Y181C variant, EC_{50}s = 1.2 and 5.0 μM against the K103N and Y188L strains, respectively. In comparison with **2**−**4**, **6g**, which was equally or less active against the wt virus but displayed slightly lower (vs **3** and **4**) or higher (vs **2**) potency against the K103N strain, was 7-fold more potent than **4** against Y181C and showed against the Y188L mutant an intermediate inhibition value between those of **2**/**3** and **4**. When compared to **5**, **6g** was 4-fold more efficient in inhibiting wt HIV-1. In respect to NVP and EFZ, **6g** was clearly more potent than NVP and showed similar activities as EFZ against wt HIV-1 and the Y181C variant, whereas it was 3-fold less active against the K103N and Y188L mutant strains.

Enzyme data are in agreement with the cellular ones. When screened against the wt RT and a panel of mutated RTs (K103N, Y181I, and L100I), **6g** together with its 4-fluoro- and 4-methoxy-analogues **6h**,**i** showed the highest inhibitory activities joined with the lowest fold resistance ratio. In comparison with **2**−**4** and EFZ, compounds **6g**−**i** showed similar (vs **3**, **4**, and EFZ) or one magnitude order lower (vs **2**) potency against wt RT, were 6- to 54-fold more efficient than **2**−**4** and EFZ against the K103N mutated RT and displayed lower potency that EFZ and higher potency than **2**−**4** against the Y181I RT.

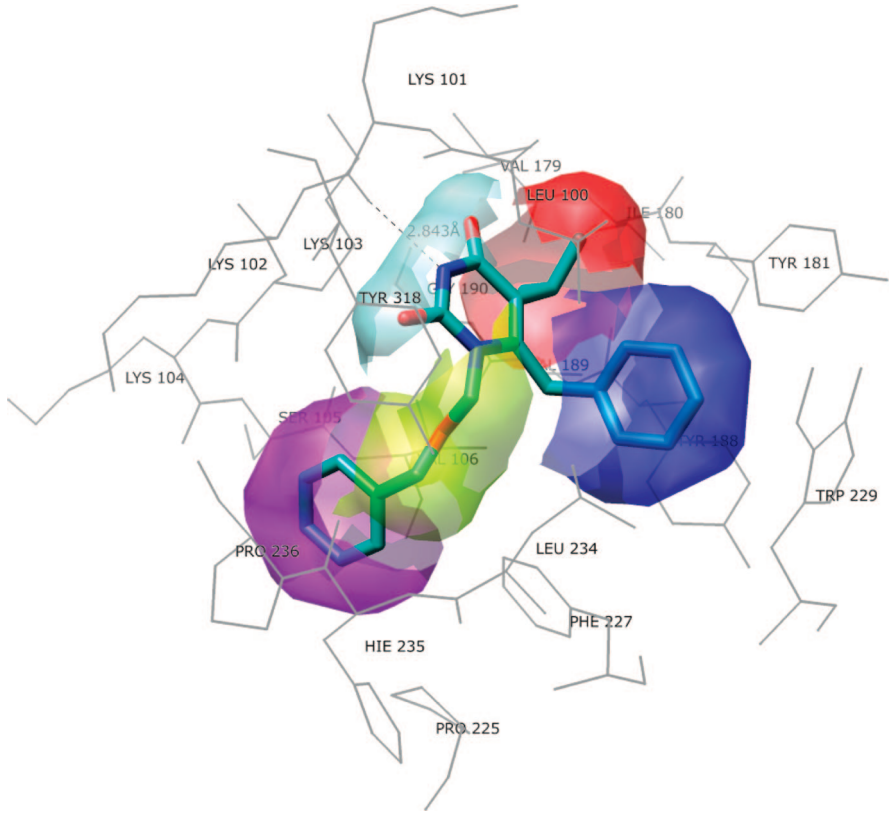

Figure 5. Experimental bound TNK-651. The WT RT is shown in gray wire. The five RT/TNK-651 interaction regions are also displayed.

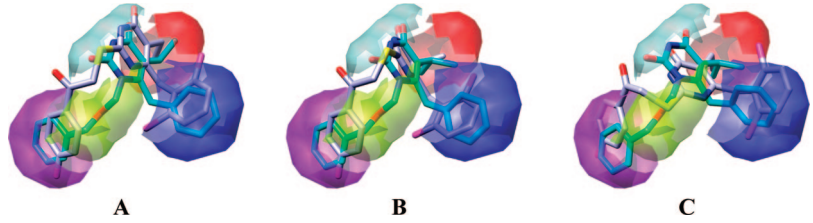

Figure 6. Derivative **6h** (pale-purple-colored carbon atoms) docked into WT (A), Y181C (B), and L100I (C) reverse transcriptases. For comparison purposes, the experimental bound conformation of TNK-651 (cyan-colored carbon atoms) is shown in stick representation. The five RT/TNK-651 interaction regions are also displayed for comparison.

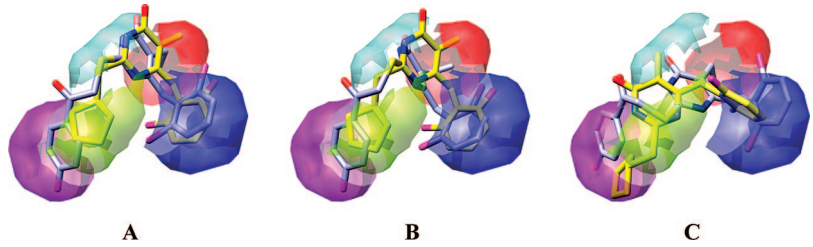

Figure 7. Derivative **6h** (pale purple) docked into WT (A), Y181C (B) and L100I (C) reverse transcriptases. For comparison purposes, the docked conformation of MC922 (yellow), an earlier F_2-*S*-DABO, is shown in stick representation. The five RT/TNK-651 interaction regions are also displayed for comparison.

Molecular modeling and binding mode studies on both wt and mutated (Y181C and L100I) RTs could, at least in part, explain the peculiar, HEPT-like SAR observed with the oxophenethyl-*S*-DABOs. In previous molecular modeling studies, we highlighted the differences between the binding modes of F_2-*S*-DABOs/F_2-*NH*-DABOs and the experimental bound conformation of the HEPT derivative TNK-651 in both WT and Y181C RTs. With the oxophenethyl-*S*-DABOs, a fair superimposition between their putative binding modes and those of TNK-651 in WT and Y181C RTs has been observed. Moreover, some differences in the binding modes of **6**−**8** and the F_2-*S*-DABO MC922 in both the enzyme structures have been found.

Experimental Section

Chemistry. Melting points were determined on a Buchi 530 melting point apparatus and are uncorrected. ^{1}H NMR and ^{13}C NMR spectra were recorded at 400 MHz on a Bruker AC 400 or at 300 MHz on a Varian Mercury 300 BB spectrometer; chemical shifts are reported in δ (ppm) units relative to the internal reference tetramethylsilane (Me_4Si) or hexamethyldisiloxane [$(Me_3Si)_2O$]. All

compounds were routinely checked by TLC and ^{1}H NMR. Mass spectra were obtained on a Agilent MS/5975 mass spectrometer. TLC was performed on aluminum-backed silica gel plates [Merck DC, Alufolien Kieselgel 60 F_{254} or AlUGRAM Nano-SIL G/UV$_{254}$ (MACHEREY-NAGEL GmbH & Co. KG)] with spots visualized by UV light. All solvents were reagent grade and, when necessary, were purified and dried by standard methods. Concentration of solutions after reactions and extractions involved the use of a rotary evaporator operating at reduced pressure of ca. 20 Torr. Organic solutions were dried over anhydrous sodium sulfate. Analytical results are within ±0.40% of the theoretical values. All chemicals were purchased from Aldrich Chimica, Milan (Italy), or from Lancaster Synthesis GmbH, Milan (Italy), and were of the highest purity. The specific examples presented below illustrate general synthetic methods. As a rule, samples prepared for physical (Table 2) and biological studies (Tables 1, 3–5) were dried in high vacuum over P_2O_5 for 20 h at temperatures ranging from 25 to 110 °C, depending on the sample melting point.

General Procedure (Scheme 1, Route a) for the Preparation of Ethyl 4-(2,6-Dihalophenyl)-3-oxobutanoates (9a,e,j) and Ethyl 4-(2,6-Dihalophenyl)-2-methyl-3-oxobutanoates (9b,f) (Example: Ethyl 4-(2-Chloro-6-fluorophenyl)-3-oxobutanoate (9e)). Triethylamine (13.4 mL, 96 mmol) and magnesium chloride (7.14 g, 75 mmol) were added to a stirred suspension of potassium malonate monoethyl ester (10.7 g, 63 mmol) in dry acetonitrile (200 mL), and stirring was continued at room temperature for 2 h. Then, a solution of the 2-chloro-6-fluorophenylacetic imidazolide in the same solvent (50 mL), prepared 15 min before by reaction between 2-chloro-6-fluorophenylacetic acid (5.66 g, 30 mmol) and *N,N′*-carbonyldiimidazole (5.84 g, 36 mmol) in acetonitrile (50 mL), was added. The reaction mixture was stirred overnight at room temperature and then was heated at reflux for 2 h. After the mixture was cooled, 13% HCl (400 mL) was cautiously added while the temperature was kept below 25 °C, and the resulting clear mixture was stirred for a further 15 min. The organic layer was separated and evaporated, and the residue was treated with ethyl acetate (200 mL). The aqueous layer was extracted with ethyl acetate (3 × 150 mL), and the organic phases were collected, washed with a sodium hydrogen carbonate saturated solution (3 × 150 mL) and brine (3 × 150 mL), dried, and concentrated to give the pure desired product as a solid, which was directly used in the following step. ^{1}H NMR ($CDCl_3$): δ 1.19 (t, 3H, OCH_2CH_3), 3.35 (s, 2H, $COCH_2CO$), 4.13 (m, 2H, OCH_2CH_3), 4.18 (s, 2H, Ar−CH_2), 7.02 (m, 1H, C_4−Ar-*H*), 7.25 (m, 2H, $C_{3,5}$−Ar-*H*). Anal. C, H, Cl, F.

General Procedure (Scheme 1, Route b) for the Preparation of Ethyl 2-Alkyl-4-(2,6-dihalophenyl)-3-oxobutanoates (9c,d,g−i,k,l) (Example: Ethyl 4-(2-Chloro-6-fluorophenyl)-3-oxo-2-iso-propylbutanoate (9h)). A few drops of ethyl 2-bromo-3-methylbutanoate were added to a vigorously stirred, boiling mixture of freshly prepared zinc turnings (50 g, 0.765 g-atom) and a trace of mercury(II) chloride in absolute THF (150 mL). After the appearance of the greenish color (5−7 min), the solution of 2-(2-chloro-6-fluorophenyl)acetonitrile (19.2 g, 113 mmol) in absolute THF (170 mL) was added. The remaining ethyl 2-bromo-3-methylbutanoate (118.5 g, 567 mmol) was added dropwise to the resulting refluxing mixture over a period of 2 h. After all the bromoester was added, the mixture was stirred and refluxed for 30 min more, the organic layer was decanted, and the unreacted zinc (14.1 g) was washed with several portions of anhydrous THF. The combined THF solutions were evaporated at slightly reduced pressure, thus living the viscous residue, which was taken up in toluene (500 mL) and quenched with 13% HCl (240 mL). The resulting mixture was stirred for 2.5 h, and the organic solution was washed with water, dried over $MgSO_4$, filtered through a silica gel pad, and evaporated under reduced pressure. The remaining oil was fractionated in vacuo on a Vigreux column to give the title product **9h** as a pale-yellow oil. H^1 NMR ($CDCl_3$): δ 0.87 (t, 6H, J = 6.84 Hz, $CH(CH_3)_2$), 1.14 (m, 3H, OCH_2CH_3), 2.38 (m, 1H, $CH(CH_3)_2$), 3.28 (dd, 1H, J_1 = 1.71 Hz, J_2 = 7.69 Hz, COCHCO), 3.94 (d, 2H, J = 10.26 Hz, ArCH_2), 4.07 (q, 2H, J_1 = 7.69 Hz, J_2 = 6.84 Hz, OCH_2CH_3), 6.84 (m, 1H, C_4−Ar-*H*), 7.05 (m, 2H, $C_{3,5}$−Ar-*H*). Anal. C, H, Cl, F.

General Procedure (Scheme 1, Route c) for the Preparation of 5-Alkyl-6-(2,6-dihalobenzyl)-2-thioxo-2,3-dihydropyrimidin-4(1*H*)-ones (10c−i) (Example: 6-(2-chloro-6-fluorobenzyl)-5-iso-propyl-2-thioxo-2,3-dihydropyrimidin-4(1*H*)-one (10h)). Absolute ethanol (110 mL) was placed in a 500 mL round-bottom flask, and potassium (3.7 g, 94.9 mg-atom) was added to the above in small pieces. Then, thiourea (3.1 g, 40.7 mmol) and ethyl 4-(2-chloro-6-fluorophenyl)-3-oxo-2-*iso*-propylbutanoate (**9h**) (5.6 g, 15.6 mmol) were subsequently added. The resulting mixture was refluxed for 90 h on oil bath and the excess solvent was distilled at normal pressure. The residue was dissolved in hot water (400 mL), and the resulting solution was boiled with 0.5 g of charcoal (30 min), cooled to room temperature, and filtered on a Buchner funnel. The filtrate was extracted with diethyl ether (3 × 25 mL), acidified to pH 4−5 with glacial acetic acid, and the resulting precipitate was filtered off, washed with water (50 mL) and diethyl ether (3 × 15 mL), and air-dried. The dry product was dissolved in boiling ethanol (50 mL), treated with 0.5 g of charcoal and filtered. The filtrate was concentrated at normal pressure, then the solution was chilled to room temperature and the separated crystals were filtered off and washed with a little cold ethanol. ^{1}H NMR (DMSO-d_6): 0.81 (d, J = 6.72 Hz, 6H, $CH(CH_3)_2$), 2.35−2.44 (m, 1H, $CH(CH_3)_2$), 3.99 (s, 2H, CH_2Ar), 7.15−7.22 (m, 1H, C_4−Ar-*H*), 7.30−7.37 (m, 2H, $C_{3,5}$−Ar-*H*), 12.24 (s, 1H, NH), 12.27 (s, 1H, NH). Anal. C, H, Cl, F, N, S.

General Procedure (Scheme 1, Route d) for the Preparation of 5-Alkyl-6-(2,6-dihalobenzyl)-2-(2-aryl-2-oxoethylsulfanyl)pyrimidin-4(3*H*)-ones (6, 7) (Example: 6-(2,6-dichlorobenzyl)-2-(2-oxo-2-phenylethylsulfanyl)pyrimidin-4(3*H*)-one (6a)). 6-(2,6-Dichlorobenzyl)-2-thioxo-2,3-dihydropyrimidin-4(1*H*)-one[13] (0.5 g, 1.74 mmol) was added in one portion to a magnetically stirred 1 M methanolic solution of sodium methoxide (0.19 g, 3.48 mmol), and stirring was continued until a clear solution was obtained. 2-Bromo-1-phenylethanone (0.36 g, 1.83 mmol) was added to this solution, and a few minutes later, a bulky, white precipitate was deposited. The mixture was quenched with 1 N acetic acid (to pH = 4) and filtered. The filter cake was washed with water, sucked dry, and recrystallized from ethanol/*N,N*-dimethylformamide (2:1) mixture. ^{1}H NMR (DMSO-d_6): δ 3.88 (s, 2H, ArCH_2), 4.64 (s, 2H, SCH_2), 5.71 (s, 1H, C_5−H), 7.15 (m, 3H, C_{3-5}−Ar-*H*), 7.53 (m, 2H, $C_{3,5}$−Ph-*H*), 7.65 (t, 1H, J = 7.33 Hz, C_4−Ph-*H*), 7.88 (d, 2H, J = 7.33 Hz, $C_{2,6}$−Ph-*H*). ^{13}C NMR (DMSO-d_6): δ 24.9 (CH_2), 33.5 (SCH_2), 114.2 (C-5), 126.9 (2C, dichlorophenyl ring), 128.3 (1C, dichlorophenyl ring), 128.6 (2C, Ph), 128.8 (2C, Ph), 132.9 (1C, Ph), 135.9 (2C, dichlorophenyl ring), 137.5 (1C, Ph), 138.6 (1C, dichlorophenyl ring), 153.4 (C-6), 162.2 (C-2), 167.9 (C-4), 194.3 (C═O). MS (EI) m/z 404 (M^+). Anal. C, H, Cl, F, N, S.

General Procedure (Scheme 1, Route e) for the Preparation of 5-Alkyl-6-(2,6-difluorobenzyl)-2-(2-aryl-2-oxoethylsulfanyl)pyrimidin-4(3*H*)-ones (8) (Example: 6-(2,6-Difluorobenzyl)-5-ethyl-2-(2-oxo-2-phenylethylsulfanyl)pyrimidin-4(3*H*)-one (8d)). Anhydrous potassium carbonate (0.13 g, 0.97 mmol) and 2-bromo-1-phenylethanone (0.19 g, 0.97 mmol) were added in succession to a suspension of 6-(2,6-difluorobenzyl)-5-ethyl-2-thioxo-2,3-dihydropyrimidin-4(1*H*)-one[15] (0.25 g, 0.88 mmol) in dry *N,N*-dimethylformamide (1.0 mL). After stirring for 5 h at room temperature, the mixture was quenched with water (10 mL) and filtered. The obtained solid residue was crystallized to furnish pure **8d**. ^{1}H NMR (DMSO-d_6): δ 0.98 (t, 3H, CH_2CH_3), 2.43 (q, 2H, CH_2CH_3), 3.77 (s, 2H, C6−CH_2), 4.47 (s, 2H, SCH_2CO), 6.64 (m, 2H, $C_{3,5}$−Ar-*H*), 6.99 (m, 1H, C_4−Ar-*H*), 7.51−7.77 (m, 5H, Ph-*H*), 12.65 (s 1H, NH). ^{13}C NMR (DMSO-d_6): δ 10.9 (CH_3), 15.4 (CH_2), 17.8 (CH_2), 33.7 (SCH_2), 111.5 (2C, difluorophenyl ring), 111.8 (1C, difluorophenyl ring), 128.3 (C-5), 128.7 (2C, Ph), 128.9 (2C, Ph), 129.1 (1C, difluorophenyl ring), 132.9 (1C, Ph), 137.4 (1C, Ph), 145.1 (C-6), 159.9 (C-2), 163.5 (C-4), 164.7 (2C, difluorophenyl ring), 193.9 (C═O). MS (EI) m/z 400 (M^+). Anal. C, H, F, N, S.

Biology. Anti-HIV Activity in Lymphoid Cells. Biological activity of the compounds was tested in the lymphoid MT-4 cell line (received from the NIH AIDS Reagent Program) against the wt HIV-1 NL4-3 strain and three different HIV-1 strains, as described before.[42–44] Briefly, MT-4 cells were infected with the appropriate HIV-1 strain (or mock-infected to determine cytotoxicity) in the presence of different drug concentrations. At day five postinfection, a tetrazolium-based colorimetric method (MTT method) was used to evaluate the number of viable cells. The HIV-1 K103N, Y181C, or Y188L mutant were received from the Medical Research Council Centralised Facility for AIDS Reagents, Herfordshire, UK.

Anti-HIV Reverse Transcriptase Assays. RNA-dependent DNA polymerase activity was assayed as described[45] in the presence of 0.5 μg of poly(rA)/oligo(dT)$_{10:1}$ (0.3 μM 3′-OH ends), 10 μM [3H]-dTTP (1 Ci/mmol), and 2−4 nM RT in the presence of 8% final concentration of DMSO.

Reagents. [^{3}H]-dTTP (40 Ci/mmol) was from Amersham and unlabeled dNTP's from Boehringer. Whatman was the supplier of the GF/C filters. All other reagents were of analytical grade and purchased from Merck or Fluka. The homopolymer poly(rA) (Pharmacia) was mixed at weight ratios in nucleotides of 10:1 to the oligomer oligo(dT)$_{12-18}$ (Pharmacia) in 20 mM Tris-HCl (pH 8.0), containing 20 mM KCl and 1 mM EDTA, heated at 65 °C for 5 min and then slowly cooled at room temperature.

Proteins. Recombinant proteins expression and purification was as described.[45] All enzymes were purified to >95% purity.

RT Inhibition Assays. Time-dependent incorporation of radioactive nucleotides into poly(rA)/oligo(dT)$_{10:1}$ at different nucleotide substrate concentrations was monitored by removing 25 μL aliquots at 2 min time intervals. Initial velocities of the reaction were then plotted against the corresponding substrate concentrations. For inhibition constant (ID_{50}) determination, an interval of inhibitor concentrations between 0.2 ID_{50} and 5 ID_{50} was used in the inhibition assays. ID_{50} values were determined with computer-aided curve fitting of the experimental data to a fully noncompetitive model. Curve fitting was performed with the program GraphPad Prism 3.0.

Molecular Modeling. RT Structure Preparation. The WT (1RT2), Y181C (1JLA) and L100I (1S1V) X-ray crystal structures of RTs complexed with TNK-651 were retrieved from the Protein Data Bank.[46–48] All the complexes were superimposed each other arbitrarily using the WT RT as reference complex. The superimposition of the RT complexes was performed by the means of the program ProFit version 2.2[49] using the implemented McLachlan algorithm.[50] All residue's backbone atoms comprised in a 20 Å core from TNK-651 were selected with the Chimera program[51] (182 residues) and used as reference for the fitting. The same number of residues (Trp88A-Tyr115A, Ser156A-Leu210A, Trp212A, Leu214A-Ile244A, Lys263A, Asn265A-Tyr271A, Glu312A-Ile326A, Tyr339A-Thr351A, Ile375A, Thr377A-Lys385A, Gln23B, Pro25B-Glu28B, Ile31B-Lys32B, Val35B, Thr131B-Arg143B) was used for all complexes superimpositions. Then, using the AMBER 8.0 suite,[52] the complexes were minimized to alleviate steric contacts that usually arise due to the random way in which hydrogens are added to the heavy atoms. Hydrogens were added to the receptors with the tLeap module. Protonation states were assumed to be those most common at pH 7, i.e., lysines, arginines, histidines, aspartates, and glutamates were considered in the ionized form. Each complex was solvated (SOLVATEOCT command) with water molecules (TIP3 model) in a box extending 10 Å and counterions were added to neutralization. The solvated complex was then refined by minimization using the SANDER module of AMBER. The parameters for the cocrystallized NNRTIs were calculated using the antechamber module of AMBER, and the atomic charges were calculated using the AM1 Hamiltonian. Once the minimizations were complete, the ligands (NNRTIs) and the receptors (RTs) were extracted into separate files (locks and keys) to be used for the subsequent docking set up.

Docking Set-Up. Autodock 4.0.1[40,53–55] was used for all docking calculations. The AutodockTools package version 1.5.0 was employed to generate the docking input files and to analyze the docking results, the same procedure as described in the manual were followed. All the nonpolar hydrogens and the water molecules were removed. The AMBER 8.0 atomic charges were saved for either the proteins or the ligands, and the prepare_receptor4.py and the prepare_ligand4.py ADT scripts were used to transform in the united atom paradigm. A grid box size of 58 × 76 × 66 points with a spacing of 0.375 Å between the grid points was implemented and extended more than 6 Å out of the NNBS. The grid was centered on the mass center of the experimental bound TNK-651 coordinates. For all the inhibitors, the single bonds including the amide bonds were treated as active torsional bonds. One hundred docked structures, i.e., 100 runs, were generated by using genetic algorithm searches. A default protocol was applied, with an initial population of 50 randomly placed individuals, a maximum number of 2.5×10^5 energy evaluations, and a maximum number of 2.7×10^4 generations. A mutation rate of 0.02 and a crossover rate of 0.8 were used. Results differing by less than 2.0 Å in positional root-mean-square deviation (rmsd) were clustered together and represented by the result with the most favorable free energy of binding. As previously reported for the Autodock 3 version,[56] the actual one (Autodock 4) proved to reproduce with lower rmsd values the experimental structures of TNK-651 (0.53, 0.59, and 0.72 rmsd values for 1RT2, 1JLA and 1S1V, respectively). The same preparation and docking protocols were applied also for the delavirdine/RT complex (PDB entry code 1KLM), which was used for comparison purposed. The structures of the newly synthesized *S*-DABOs were drawn by the mean of the jchempaint (http://jchempaint.sourceforge.net/) software,[57] converted into three-dimensional structure using the CDK libraries,[58,59] and subsequently optimized with the sander module of the AMBER8 suite. The needed parameters to run the sander minimization were calculated using the antechamber module similarly as reported above. The docking results for each of the three enzyme isoforms (WT, L100I, and Y181C) were then clustered using a rmsd tolerance value of 2.0. In each cluster, the best cluster conformation was coincident with the best docked.[56]

Acknowledgment. This work was partially supported by the EU Contract LSHB-CT-2003-503480-TRIoH (to G.M. and J.A.E.) and the Spanish MEC project BFU2006-00966 and FIS PI060624 (J.A.E.). I. Clotet-Codina holds a FI scholarship from Generalitat de Catalunya. S. Zanoli is recipient of a Fondazione Buzzati-Traverso Fellowship.

Supporting Information Available: Chemical and physical data of compounds **1a**−**p**. Elemental analyses of compounds **1**, **6**−**8**. ^{1}H NMR, ^{13}C NMR, and MS (EI) data for compounds **6**−**8**. Figures S1−S6 (Molecular Modeling Section). This material is available free of charge via the Internet at http://pubs.acs.org.

References

(1) Artico, M. Selected non-nucleoside reverse transcriptase inhibitors (NNRTIs): the DABOs family. *Drug Future* **2002**, *27*, 159–175.
(2) Marongiu, M. E.; Pani, A.; Musiu, C.; La Colla, P.; Mai, A.; Sbardella, G.; Massa, S.; Artico, M. 3,4-Dihydro-2-alkoxy-6-benzyl-oxopyrimidines (DABOs): Development of a potent class of non-nucleoside reverse transcriptase inhibitors. *Recent Res. Dev. Med. Chem.* **2001**, *1*, 65–92.
(3) De Clercq, E. Emerging anti-HIV drugs. *Expert Opin. Emerging Drugs* **2005**, *10*, 241–273.
(4) De Clercq, E. New Approaches toward Anti-HIV Chemotherapy. *J. Med. Chem.* **2005**, *48*, 1297–1313.
(5) Campiani, G.; Ramunno, A.; Maga, G.; Nacci, V.; Fattorusso, C.; Catanalotti, E.; Morelli, E.; Novellino, E. Non-nucleoside HIV-1 reverse transcriptase (RT) inhibitors: past, present, and future perspectives. *Curr. Pharm. Des.* **2002**, *8*, 615–657.
(6) Botta, M.; Artico, M.; Massa, S.; Gambacorta, A.; Marongiu, M. E.; Pani, A.; La Colla, P. Synthesis, Antimicrobial and Antiviral Activities of Isotrimethoprim and Some Related Derivatives. *Eur. J. Med. Chem.* **1992**, *27*, 251–257.
(7) Artico, M.; Massa, S.; Mai, A.; Marongiu, M. E.; Piras, G.; Tramontano, E.; La Colla, P. 3,4-Dihydro-2-alkoxy-6-benzyl-4-oxopyrimidines (DABOs): a New Class of Specific Inhibitors of

Human Immunodeficiency Virus Type 1. *Antiviral Chem. Chemother.* **1993**, *4*, 361–368.
(8) Tramontano, E.; Marongiu, M. E.; De Montis, A.; Loi, A. G.; Artico, M.; Massa, S.; Mai, A.; La Colla, P. Characterization of the Anti-HIV-1 Activity of 3,4-Dihydro-2-alkoxy-6-benzyl-4-oxopyrimidines (DABOs), New Non-Nucleoside Reverse Transcriptase Inhibitors. *Microbiologica* **1994**, *17*, 269–279.
(9) Massa, S.; Mai, A.; Artico, M.; Sbardella, G.; Tramontano, E.; Loi, A. G.; Scano, P.; La Colla, P. Synthesis and antiviral activity of new 3,4-dihydro-2-alkoxy-6-benzyl-4-oxopyrimidines (DABOs), specific inhibitors of human immunodeficiency virus Type-1. *Antiviral Chem. Chemother.* **1995**, *6*, 1–8.
(10) Mai, A.; Artico, M.; Sbardella, G.; Massa, S.; Loi, A. G.; Tramontano, E.; Scano, P.; La Colla, P. Synthesis and anti-HIV-1 Activity of Thio Analogues of Dihydroalkoxybenzyloxopyrimidines. *J. Med. Chem.* **1995**, *38*, 3258–3263.
(11) Ettorre, A.; Mai, A.; Artico, M.; Massa, S.; De Montis, A.; La Colla, P. 6-(3-Methylbenzyl)-2-(2-methylpropyl)thio-4(3*H*)-pyrimidinone (DABO 622). *Acta Crystallogr., Sect. C: Cryst. Struct. Commun.* **1996**, *52*, 2115–2117.
(12) Mai, A.; Artico, M.; Sbardella, G.; Quartarone, S.; Massa, S.; Loi, A. G.; De Montis, A.; Scintu, F.; Putzolu, M.; La Colla, P. Dihydro(alkylthio)(naphthylmethyl)oxopyrimidines: Novel Non-Nucleoside Reverse Transcriptase Inhibitors of the *S*-DABO Series. *J. Med. Chem.* **1997**, *40*, 1447–1454.
(13) Mai, A.; Artico, M.; Sbardella, G.; Massa, S.; Novellino, E.; Greco, G.; Loi, A. G.; Tramontano, E.; Marongiu, M. E.; La Colla, P. 5-Alkyl-2-(alkylthio)-6-(2,6-dihalophenylmethyl)-3,4-dihydropyrimidin-4(3*H*)-ones: Novel Potent and Selective Dihydro-alkoxy-benzyl-oxopyrimidine Derivatives. *J. Med. Chem.* **1999**, *42*, 619–627.
(14) Sbardella, G.; Mai, A.; Artico, M.; Massa, S.; Marceddu, T.; Vargiu, L.; Marongiu, M. E.; La Colla, P. Does the 2-Methylthiomethyl Substituent Really Confer High Anti-HIV-1 Activity to S-DABOs. *Med. Chem. Res.* **2000**, *10*, 30–39.
(15) Sbardella, G.; Mai, A.; Artico, M.; Chimenti, P.; Massa, S.; Loddo, R.; Marongiu, M. E.; La Colla, P.; Pani, A. Structure−activity relationship studies on new DABOs: effect of substitutions at pyrimidine C-5 and C-6 positions on anti-HIV-1 activity. *Antiviral Chem. Chemother.* **2001**, *12*, 37–50.
(16) Pani, A.; Musiu, C.; Loi, A. G.; Mai, A.; Loddo, R.; La Colla, P.; Marongiu, M. E. DABOs as candidates to prevent mucosal HIV transmission. *Antiviral Chem. Chemother.* **2001**, *12*, 51–59.
(17) Mai, A.; Sbardella, G.; Artico, M.; Ragno, R.; Massa, S.; Novellino, E.; Greco, G.; Lavecchia, A.; Musiu, C.; La Colla, M.; Murgioni, C.; La Colla, P.; Loddo, R. Structure-based Design, Synthesis, and Biological Evaluation of Conformationally Restricted Novel 2-Alkylthio-6-[1-(2,6-difluorophenyl)alkyl]-3,4-dihydro-5-alkylpyrimidin-4(3*H*)-ones as Non-nucleoside Inhibitors of HIV-1 Reverse Transcriptase. *J. Med. Chem.* **2001**, *44*, 2544–2554.
(18) Quaglia, M. G.; Mai, A.; Sbardella, G.; Artico, M.; Ragno, R.; Massa, S.; Del Piano, D.; Setzu, G.; Doratiotto, S.; Cotichini, V. Chiral Resolution and Molecular Modeling Investigation of *rac*-2-Cyclopentylthio-6-[1-(2,6-difluorophenyl)ethyl]-3,4-dihydro-5-methylpyrimidin-4(3*H*)-one (MC-1047), a Potent Anti-HIV-1 Reverse Transcriptase Agent of the DABO Class. *Chirality* **2001**, *13*, 75–80.
(19) Ragno, R.; Mai, A.; Sbardella, S.; Artico, M.; Massa, S.; Musiu, C.; Mura, M.; Marceddu, T.; Cadeddu, A.; La Colla, P. Computer-aided design, synthesis, and anti-HIV-1 activity in vitro of 2-alkylamino-6-[1-(2,6-difluorophenyl)alkyl]-3,4-dihydro-5-alkylpyrimidin-4(3*H*)-ones as novel potent non-nucleoside reverse transcriptase inhibitors, also active against the Y181C variant. *J. Med. Chem.* **2004**, *47*, 928–934.
(20) Mai, A.; Artico, M.; Ragno, R.; Sbardella, G.; Massa, S.; Musiu, C.; Mura, M.; Marturana, F.; Cadeddu, A.; Maga, G.; La Colla, P. 5-Alkyl-2-alkylamino-6-(2,6-difluorophenylalkyl)-3,4-dihydropyrimidin-4(3*H*)-ones, a new series of potent, broad-spectrum non-nucleoside reverse transcriptase inhibitors belonging to the DABO family. *Bioorg. Med. Chem.* **2005**, *13*, 2065–2077.
(21) Cancio, R.; Mai, A.; Rotili, D.; Artico, M.; Sbardella, G.; Clotet-Codina, I.; Esté, J. A.; Crespan, E.; Zanoli, S.; Hübscher, U.; Spadari, S.; Maga, G. Slow-, Tight-Binding HIV-1 Reverse Transcriptase Non-Nucleoside Inhibitors Highly Active against Drug-Resistant Mutants. *ChemMedChem* **2007**, *2*, 445–448.
(22) Mai, A.; Artico, M.; Rotili, D.; Tarantino, D.; Clotet-Codina, I.; Armand-Ugón, M.; Ragno, R.; Simeoni, S.; Sbardella, G.; Nawrozkij, M. B.; Samuele, A.; Maga, G.; Esté, J. A. Synthesis and Biological Properties of Novel 2-Aminopyrimidin-4(3*H*)-ones Highly Potent Against HIV-1 Mutant Strains. *J. Med. Chem.* **2007**, *50*, 5412–5424.
(23) Baba, M.; Tanaka, H.; De Clercq, E.; Pauwels, R.; Balzarini, J.; Schols, D.; Nakashima, H.; Perno, C.-F.; Walker, R. T.; Miyasaka, T. Highly specific inhibition of human immunodeficiency virus type 1 by a novel 6-substituted acyclouridine derivative. *Biochem. Biophys. Res. Commun.* **1989**, *165*, 1375–1381.
(24) Miyasaka, T.; Tanaka, H.; Baba, M.; Hayakawa, H.; Walker, R. T.; Balzarini, J.; De Clercq, E. A novel lead for specific anti-HIV-1 agents: 1-[(2-hydroxyethoxy)methyl]-6-(phenylthio)thymine. *J. Med. Chem.* **1989**, *32*, 2507–2509.
(25) Yuasa, S.; Sadakata, Y.; Takashima, H.; Sekiya, K.; Inouye, N.; Ubasawa, M.; Baba, M. Selective and synergistic inhibition of human immunodeficiency virus type 1 reverse transcriptase by a non-nucleoside inhibitor, MKC-442. *Mol. Pharmacol.* **1993**, *44*, 895–900.
(26) Baba, M.; Shigeta, S.; Yuasa, S.; Takashima, H.; Sekiya, K.; Ubasawa, M.; Tanaka, H.; Miyasaka, T.; Walker, R. T.; De Clercq, E. Preclinical evaluation of MKC-442, a highly potent and specific inhibitor of human immunodeficiency virus type 1 in vitro. *Antimicrob. Agents Chemother.* **1994**, *38*, 688–692.
(27) Tanaka, H.; Takashima, H.; Ubasawa, M.; Sekiya, K.; Inouye, N.; Baba, M.; Shigeta, S.; Walker, R. T.; De Clercq, E.; Miyasaka, T. Synthesis and antiviral activity of 6-benzyl analogs of 1-[(2-hydroxyethoxy)methyl]-6-(phenylthio)thymine (HEPT) as potent and selective anti-HIV-1 agents. *J. Med. Chem.* **1995**, *38*, 2860–2865.
(28) Hopkins, A. L.; Ren, J.; Tanaka, H.; Baba, M.; Okamato, M.; Stuart, D. I.; Stammers, D. K. Design of MKC-442 (emivirine) analogues with improved activity against drug-resistant HIV mutants. *J. Med. Chem.* **1999**, *42*, 4500–4505.
(29) The arylalkyl-*S*-DABOs **1a**−**p** were prepared by alkylation of the proper 2-thiouracil and -thiothymine with the opportune arylalkyl halide according to our reported procedure.[13] The physical and chemical data for compounds **1a**−**p** have been reported in Table S1 as Supporting Information. Compounds **1q**,**r**, here reported for a direct comparison as reference drugs, were described in ref 13.
(30) Mugnaini, C.; Manetti, F.; Esté, J. A.; Clotet-Codina, I.; Maga, G.; Cancio, R.; Botta, M.; Corelli, F. Synthesis and biological investigation of *S*-aryl-*S*-DABO derivatives as HIV-1 inhibitors. *Bioorg. Med. Chem. Lett.* **2006**, *16*, 3541–3544.
(31) Manetti, F.; Estè, J. A.; Clotet-Codina, I.; Armand-Ugòn, M.; Maga, G.; Crespan, E.; Cancio, R.; Mugnaini, C.; Bernardini, C.; Togninelli, A.; Carmi, C.; Alongi, M.; Petricci, E.; Massa, S.; Corelli, F.; Botta, M. Parallel Solution-Phase and Microwave-Assisted Synthesis of New *S*-DABO Derivatives Endowed with Subnanomolar Anti-HIV-1 Activity. *J. Med. Chem.* **2005**, *48*, 8000–8008.
(32) Mugnaini, C.; Alongi, M.; Togninelli, A.; Gevarija, H.; Brizzi, A.; Manetti, F.; Bernardini, C.; Angeli, L.; Tafi, A.; Bellucci, L.; Corelli, F.; Massa, S.; Maga, G.; Samuele, A.; Facchini, M.; Clotet-Codina, I.; Armand-Ugón, M.; Esté, J. A.; Botta, M. Dihydro-alkylthio-benzyl-oxopyrimidines as Inhibitors of Reverse Transcriptase: Synthesis and Rationalization of the Biological Data on Both Wild-Type Enzyme and Relevant Clinical Mutants. *J. Med. Chem.* **2007**, *50*, 6580–6505.
(33) He, Y.; Chen, F.; Sun, G.; Wang, Y.; De Clercq, E.; Balzarini, J.; Pannecouque, C. 5-Alkyl-2-[(aryl and lakyloxylcarbonylmethyl)thio]-6-(1-naphthylmethyl) pyrimidin-4(3*H*)-ones as an unique HIV reverse transcriptase inhibitors of *S*-DABO series. *Bioorg. Med. Chem. Lett.* **2004**, *14*, 3173–3176.
(34) He, Y.; Chen, F.; Yu, X.; Wang, Y.; De Clercq, E.; Balzarini, J.; Pannecouque, C. Non-nucleoside HIV-1 reverse transcriptase inhibitors; part 3. Synthesis and antiviral activity of 5-alkyl-2-[(aryl and alkyloxylcarbonylmethyl)thio]-6-(1-naphthylmethyl) pyrimidin-4(3*H*)-ones. *Bioorg. Chem.* **2004**, *32*, 536–548.
(35) Brown, H. C.; Rogic, M. M.; Rathke, M. W.; Kabalka, G. W. Mono- and dialkylation of ethyl dihaloacetates by reaction with organoboranes under the influence of potassium *tert*-butoxide. Convenient procedures for the conversion of olefins into the alpha-halo alkanoic or dialkylacetic acid esters via hydroboration. *J. Am. Chem. Soc.* **1968**, *90*, 1911–1913.
(36) Hopkins, A. L.; Ren, J.; Esnouf, R. M.; Willcox, B. E.; Jones, E. Y.; Ross, C.; Miyasaka, T.; Walker, R. T.; Tanaka, H.; Stammers, D. K.; Stuart, D. I. Complexes of HIV-1 reverse transcriptase with inhibitors of the HEPT series reveal conformational changes relevant to the design of potent non-nucleoside inhibitors. *J. Med. Chem.* **1996**, *39*, 1589–1600.
(37) Deshpande, N.; Addess, K. J.; Bluhm, W. F.; Merino-Ott, J. C.; Townsend-Merino, W.; Zhang, Q.; Knezevich, C.; Xie, L.; Chen, L.; Feng, Z.; Green, R. K.; Flippen-Anderson, J. L.; Westbrook, J.; Berman, H. M.; Bourne, P. E. The RCSB Protein Data Bank: a redesigned query system and relational database based on the mmCIF schema. *Nucleic Acids Res.* **2005**, *33*, D233–D237.
(38) Ren, J.; Nichols, C.; Bird, L.; Chamberlain, P.; Weaver, K.; Short, S.; Stuart, D. I.; Stammers, D. K. Structural mechanisms of drug resistance for mutations at codons 181 and 188 in HIV-1 reverse transcriptase and the improved resilience of second generation non-nucleoside inhibitors. *J. Mol. Biol.* **2001**, *312*, 795–805.
(39) Ren, J.; Nichols, C. E.; Chamberlain, P. P.; Weaver, K. L.; Short, S. A.; Stammers, D. K. Crystal structures of HIV-1 reverse transcriptases mutated at codons 100, 106, and 108 and mechanisms of resistance to non-nucleoside inhibitors. *J. Mol. Biol.* **2004**, *336*, 569–578.

(40) Goodsell, D. S.; Morris, G. M.; Olson, A. J. Automated docking of flexible ligands: applications of AutoDock. *J. Mol. Recognit.* **1996**, *9*, 1–5.
(41) Esnouf, R. M.; Ren, J.; Hopkins, A. L.; Ross, C. K.; Jones, E. Y.; Stammers, D. K.; Stuart, D. I. Unique features in the structure of the complex between HIV-1 reverse transcriptase and the bis(heteroaryl)piperazine (BHAP) U-90152 explain resistance mutations for this non-nucleoside inhibitor. *Proc. Natl. Acad. Sci. U.S.A.* **1997**, *94*, 3984–3989.
(42) Armand-Ugon, M.; Gutierrez, A.; Clotet, B.; Esté, J. A. HIV-1 Resistance to the gp41-Dependent Fusion Inhibitor C-34. *Antiviral Res.* **2003**, *59*, 137–142.
(43) Moncunill, G.; Armand-Ugon, M.; Clotet, I.; Pauls, E.; Ballana, E.; Llano, A.; Romagnoli, B.; Vrijbloed, J. W.; Gombert, F. O.; Clotet, B.; De Marco, S.; Esté, J. A. Anti-HIV Activity and Resistance Profile of the CXCR4 Antagonist POL3026. *Mol. Pharmacol.* **2008**, *73*, 1264–1273.
(44) Moncunill, G.; Armand-Ugon, M.; Pauls, E.; Clotet, B.; Esté, J. A. HIV-1 escape to CCR5 coreceptor antagonism through selection of CXCR4-using variants in vitro. *AIDS* **2008**, *22*, 23–31.
(45) Maga, G.; Amacker, M.; Ruel, N.; Hubscher, U.; Spadari, S. Resistance to nevirapine of HIV-1 reverse transcriptase mutants: loss of stabilizing interactions and thermodynamic or steric barriers are induced by different single amino acid substitutions. *J. Mol. Biol.* **1997**, *274*, 738–747.
(46) Westbrook, J.; Feng, Z.; Chen, L.; Yang, H.; Berman, H. M. The Protein Data Bank and structural genomics. *Nucleic Acids Res.* **2003**, *31*, 489–491.
(47) Berman, H.; Henrick, K.; Nakamura, H. Announcing the Worldwide Protein Data Bank. *Nat. Struct. Biol.* **2003**, *10*, 980.
(48) Berman, H. M.; Westbrook, J.; Feng, Z.; Gilliland, G.; Bhat, T. N.; Weissig, H.; Shindyalov, I. N.; Bourne, P. E. The Protein Data Bank. *Nucleic Acids Res.* **2000**, *28*, 235–242.
(49) Martin A. C. R. *Profit 2.2*; http://www.bioinf.org.uk/software/profit/.
(50) McLachlan, A. D. Rapid comparison of protein structures. *Acta Crystallogr., Sect. A: Found. Crystallogr.* **1982**, *38*, 871–873.
(51) Pettersen, E. F.; Goddard, T. D.; Huang, C. C.; Couch, G. S.; Greenblatt, D. M.; Meng, E. C.; Ferrin, T. E. UCSF Chimera: A Visualization System for Exploratory Research and Analysis. *J. Comput. Chem.* **2004**, *25*, 1605–1612.
(52) Case, D. A.; Darden, T. A.; Cheatham, T. E., III; Simmerling, C. L.; Wang, J.; Duke, R. E.; Luo, R.; Merz, K. M.; Wang, B.; Pearlman, D. A.; Crowley, M.; Brozell, S.; Tsui, V.; Gohlke, H.; Mongan, J.; Hornak, V.; Cui, G.; Beroza, P.; Schafmeister, C.; Caldwell, J. W.; Ross, W. S.; Kollman, P. A. *AMBER 8*; University of California: San Francisco., 2004.
(53) Morris, G. M.; Goodsell, D. S.; Halliday, R. S.; Huey, R.; William, E.; Hart, W. E.; Belew, R. K.; Olson, A. J. Automated docking using a Lamarckian genetic algorithm and an empirical binding free energy function. *J. Comput. Chem.* **1998**, *19*, 1639–1662.
(54) Sousa, S. F.; Fernandes, P. A.; Ramos, M. J. Protein−ligand docking: current status and future challenges. *Proteins* **2006**, *65*, 15–26.
(55) Huey, R.; Morris, G. M.; Olson, A. J.; Goodsell, D. S. A semiempirical free energy force field with charge-based desolvation. *J. Comput. Chem.* **2007**, *28*, 1145–1152.
(56) Ragno, R.; Frasca, S.; Manetti, F.; Brizzi, A.; Massa, S. HIV-reverse transcriptase inhibition: inclusion of ligand-induced fit by cross-docking studies. *J. Med. Chem.* **2005**, *48*, 200–212.
(57) Krause, S.; Willighagen, E.; Steinbeck, C. J. ChemPaint: Using the Collaborative Forces of the Internet to Develop a Free Editor for 2D Chemical Structures. *Molecules* **2000**, *5*, 93–98.
(58) Steinbeck, C.; Hoppe, C.; Kuhn, S.; Floris, M.; Guha, R.; Willighagen, E. L. Recent developments of the chemistry development kit (CDK): an open-source Java library for chemo- and bioinformatics. *Curr. Pharm. Des.* **2006**, *12*, 2111–2120.
(59) Steinbeck, C.; Han, Y.; Kuhn, S.; Horlacher, O.; Luttmann, E.; Willighagen, E. The Chemistry Development Kit (CDK): an open-source Java library for Chemo- and Bioinformatics. *J. Chem. Inf. Comput. Sci.* **2003**, *43*, 493–500.

JM800340W